Research article

JGS
Journal of the Geological Society

https://doi.org/10.1144/jgs2023-120 | Vol. 181 | 2024 | jgs2023-120

Indicative meanings of geological sea-level indicators in the Solent region and Sussex coast (south coast of England) and implications for uplift rates

Rebecca M. Briant[1*], Martin R. Bates[2], Jenni Robertson[3], Jean-Luc Schwenninger[4] and John E. Whittaker[5,†]

[1] Department of Geography, Birkbeck, University of London, Malet Street, London WC1E 7HX, UK
[2] School of Archaeology, History and Anthropology, University of Wales Trinity Saint David, Lampeter Campus, Lampeter SA48 7ED, UK
[3] Department of Earth and Planetary Sciences, Birkbeck, University of London, Malet Street, London WC1E 7HX, UK
[4] Research Laboratory for Archaeology and the History of Art, Dyson Perrins Building, South Parks Road, Oxford OX1 3QY, UK
[5] Palaeontology Department, Natural History Museum, Cromwell Road, London SW7 5BD, UK
RMB, 0000-0003-3776-0313
* Correspondence: b.briant@bbk.ac.uk
†deceased

Abstract: The Solent Region and Sussex coastal plain in southern England have preserved palaeo-sea-level indicators from multiple interglacial periods, with a particularly complete record of deposition throughout the last interglacial. However, as yet, none of the research on these indicators has fully addressed the relationship of the different types of deposits preserved to mean sea-level. In this paper we apply recent approaches to estimating past relative sea-levels based on applying modern analogues to understand the indicative meaning of these indicators. We also apply a synchronous correlation model previously developed on rapidly uplifting coastlines to assess uplift rates. The uplift rates required to match the elevations of sequences suggest a significant decrease in uplift rates between the Late Wolstonian Substage and Ipswichian Stage; that is, the *c.* 240 and *c.* 125 ka sea-level highstands, broadly equivalent to marine isotope stages (MIS) 7 and 5e. This coincides in time with the final opening of the Straits of Dover.

Supplementary material: Fossil data from sites that have not previously been published are available at https://doi.org/10.6084/m9.figshare.c.7172532

Received 21 July 2023; **revised** 1 February 2024; **accepted** 26 March 2024

Geomorphological sea-level indicators play an important role in constraining Quaternary global sea-level estimates (e.g. Kopp *et al.* 2009; Cohen *et al.* 2022). This is particularly because they are often found in 'near-field' locations, adjacent to the ice sheets whose fluctuations drive eustatic change. Long *et al.* (2015) showed clearly that near-field locations, owing to gravitational effects, experience a very different trajectory of sea-level transgression and regression compared with far-field locations such as coral terraces. However, the complexity of natural systems and tidal regimes means that the elevation in a landscape where a feature is preserved may not represent mean sea-level. Therefore, elevations need to be corrected to give an 'indicative meaning' of former relative sea-levels (palaeo-RSL) (Rovere *et al.* 2016). This is particularly important where tidal ranges are high, as in southern England. This paper presents indicative meanings from the Solent region and Sussex coast in southern England, based on modern analogues from the same regions to provide more accurate values for future studies. Recently, various palaeo-RSL values from this region were calculated as part of the World Atlas of Last Interglacial Shorelines (WALIS) project (Cohen *et al.* 2022; Table 1), but no uplift modelling was undertaken. Although modern analogue data are preferred to calculate palaeo-RSL values (Rovere *et al.* 2016), there were none available from this region at that time. Thus all the WALIS palaeo-RSL values shown in Table 1 were corrected using a first-order approximation using the method of Lorscheid and Rovere (2019). This uses global wave and tide datasets and a series of hydro- and morphodynamic equations to calculate indicative meaning for a range of RSL indicators. Our study therefore provides an opportunity to refine these palaeo-RSL values using modern analogue data.

These relative sea-level indicators can also be used to estimate uplift rates if they have robust age control, which is present along the Sussex coast owing to a large programme of optically stimulated luminescence (OSL) dating in this region (e.g. Briant *et al.* 2006; Bates *et al.* 2010; Table 2). Previous uplift modelling (Westaway *et al.* 2006) suggested a rate of 0.134 mm a^{-1} since the formation of the Boxgrove beach mentioned below, chosen because this fitted the observed tie-points best. However, it is clear from Table 1 that the tie-points used do not represent geomorphologically meaningful features because they represent the upper surface of the deposit, which may have been modified later by erosion or the addition of overlying slope deposits or both.

The uplift modelling method applied here is synchronous correlation (Houghton *et al.* 2003; Roberts *et al.* 2009, 2013; Meschis *et al.* 2018; Pedoja *et al.* 2018; Robertson *et al.* 2019). This approach uses global sea-level curve data and measured palaeoshoreline elevations to determine where within the landscape globally identified sea-level highstands would be expected under various uplift scenarios (either constant or changing over time). Synchronous correlation modelling identifies a 'best-fit' uplift rate for the geomorphological data in a particular location through an iterative approach where at least one palaeoshoreline is correlated to a sea-level highstand using an absolute age control. This modelling is designed to use the inner edge of a marine terrace (WALIS

Table 1. Previous palaeo-sea-level estimates from Westaway et al. (2006), Kopp et al. (2009) and Cohen et al. (2022)

Sequence	Westaway *et al.* (2006)		Kopp *et al.* (2009)		World Atlas of Last Interglacial Shorelines (WALIS), Cohen *et al.* (2022)		
	Correction applied	Elevation quoted (grid references for locations not given)	Correction applied	Elevations quoted (grid references for locations not given)	Correction applied (using Lorscheid and Rovere 2019)	Type of datapoint	Elevations quoted (grid references given in WALIS database)
Marine terraces (various ages)							
Goodwood–Slindon Formation at Boxgrove	None (upper surface of deposit)	42 m OD (MIS 13a)					
Brighton–Norton Formation at Norton Farm	None (upper surface of deposit)	10 m (late MIS 7)				Marine limiting	Elevation: 11.25 ± 1.5 m
Beach deposits (various ages)							
Aldingbourne Formation at Norton Farm	None (upper surface of deposit)	25 m OD (MIS 9)			Beach deposit: IR = 3.81 RWL = 0.36	Sea-level indicator	Elevation: 21.4 ± 1.5 m 21.6 ± 1.5 m 22 ± 1.5 m Palaeo RSL: 21.04 ± 2.42 m 21.24 ± 2.42 m 21.64 ± 2.42 m
Aldingbourne Formation at Pear Tree Knap					Beach deposit: IR = 3.81 RWL = 0.36	Sea-level indicator	Elevation: 21.6 ± 1.5 m 22.4 ± 1.5 m 22.6 ± 1.5 m Palaeo RSL: 21.24 ± 2.42 m 22.04 ± 2.42 m 22.24 ± 2.42 m
Pagham Formation (PF): West Street, Selsey		4 m OD (MIS 5e)	Not clear from paper	Elevation: 4 m OD ± 1 m Palaeo RSL: 9.13 ± 8 m	na	Marine limiting	Elevation: 6.1 ± 1 m
PF: Pagham Water Treatment Works					na	Marine limiting	Elevation: 3 ± 1 m
PF: Chalcroft Nurseries					na	Marine limiting	Elevation: 6 ± 1 m 5.5 ± 1 m 5 ± 1 m 4.5 ± 1 m 3.5 ± 1 m
PF: Warblington					na	Marine limiting	Elevation: 1.2 ± 1 m
PF: Woodhorn Farm					na	Marine limiting	Elevation: 5.2 ± 1 m 6.2 ± 1 m

Continued

Table 1. *Continued*

Sequence	Westaway *et al.* (2006)		Kopp *et al.* (2009)		World Atlas of Last Interglacial Shorelines (WALIS), Cohen *et al.* (2022)		
	Correction applied	Elevation quoted (grid references for locations not given)	Correction applied	Elevations quoted (grid references for locations not given)	Correction applied (using Lorscheid and Rovere 2019)	Type of datapoint	Elevations quoted (grid references given in WALIS database)
Salt marsh and estuary deposits (Ipswichian, equivalent to MIS 5e)							
Bembridge Foreland					Saltmarsh (undifferentiated):	Sea-level indicator	Elevation: 5 ± 1 m
					IR = 2		Palaeo RSL: 4.02 ± 1.41 m
					RWL = 0.98		
Stone Point base of estuarine unit 2d in borehole 16					Tidal (brackish) mudflat:	Sea-level indicator	Elevation: −8.3 ± 0.5 m
					IR = 1.9		Palaeo RSL: −8.5 ± 2.25 m
					RWL = 1.05		
Stone Point top of estuarine unit 2d in test pit 7					Low saltmarsh environment:	Sea-level indicator	Elevation: −1.5 ± 0.5 m
					IR = 4.4		Palaeo RSL: −2.55 ± 1.07 m
					RWL = 0.2		

Indicative meaning from Cohen *et al.* (2022), following the method of Rovere *et al.* (2016). U_1 (L_1), upper (lower) range of landform in modern analogue in relation to mean sea-level; IR, indicative range = $U_1 - L_1$; RWL, reference water level = $(U_1 + L_1)/2$; E, elevation of palaeo-sea-level indicator above MSL, with error (E_e); RSL, palaeo-relative sea-level = E-RWL; δRSL, error on RSL = Sqrt $((IR/2)^2 + (E_e/2)^2)$. It should be noted that other estimates are listed in the WALIS database (https://zenodo.org/record/7944196#.ZGSlck_MKUl) reported by Cohen *et al.* (2022), with a representative sample (excluding all terrestrial limiting points) given below. na, not analysed.

Table 2. OSL age estimates from various sequences within the Sussex–Hampshire Coastal Corridor containing sea-level indicators that are listed in Table 1 and/or shown in Figure 3

Site	Stratigraphic unit	Sample code	Laboratory code	OSL dates (ka)	Original reference
Marine terraces					
Norton Farm	Brighton-Norton Formation	BH16 6.1–6.55	X1736	232.8 ± 27.4	Bates *et al.* (2010)
		BH2 3.86–3.89	X1850	147.6 ± 11.4	
Bembridge	Storm beach (see Table 4)	3, beach		121.9 ± 10.4	Wenban-Smith *et al.* (2005)
Beach deposits					
Pear Tree Knap	Aldingbourne Formation (Sands III)	PTK06-1	X2822	143.8 ± 15.3	Bates *et al.* (2010)
		PTK06-2	X2823	135.2 ± 11.2	
		PTK06-3	X2824	103.6 ± 18.4	
		PTK06-4	X2825	119.8 ± 17.7	
	Aldingbourne Formation (Silts VI)	PTK06-5	X2826	180.8 ± 17	Bates *et al.* (2010)
		PTK06-6	X2827	124 ± 26	
		PTK06-9	X2830	104.9 ± 15.9	
		PTK06-10	X2831	152.2 ± 22.7	
Selsey West Street	Pagham Formation	SEL01-1	X549	138.8 ± 11	Bates *et al.* (2010)
		SEL01-2	X550	126 ± 10.1	
Pagham Water Treatment Plant	Pagham Formation	PWT06-01	X2796	123.8 ± 8.7	Bates *et al.* (2010)
			X2797	117.4 ± 19.7	
Warblington	Pagham Formation	WAB, BH1, 6–7 m	X2875	131.7 ± 12.4	Bates *et al.* (2010)
Chalcroft Nursery	Pagham Formation	CHCN BH3, 2.6 m	X2821	195.9 ± 26.1	Bates *et al.* (2010)
		CHCN BH 3 3.3 m	X2819	231.3 ± 19.7	
		CHCN BH 3 3.8 m	X2820	582.4 ± 75.6	
		CHCN BH 2 3.95 m	X3042	233.0 ± 21.1	
		CHCN BH 24.15 m	X3043	104.4 ± 17.3	
Woodhorn Farm	Pagham Formation	WHF05 BH1 4.48–4.54 m	X2876	123.9 ± 9.6	Bates *et al.* (2010)
Butlins, Bognor	Pagham Formation	BUT 11, OSL 1	X5283	119.01 ± 12.52	Previously unpublished
North Street, Worthing	Pagham Formation	OSL 1		121.75 ± 21.07	Previously unpublished
		OSL 2		135.64 ± 8.84	
Estuarine and salt-marsh deposits					
Bembridge Foreland	See Table 2	4, salt marsh		129.1 ± 8.1	Wenban-Smith *et al.* (2005)
		5, estuary		141.3 ± 14.4	
Stone Point (bracket estuarine Ipswichian deposits)	Lepe Upper Gravel (FG)	LEPE03-05	X1729	57 ± 6	Briant *et al.* (2006)
	Lepe Lower Gravel (FG)	LEPE03-01	X1725	198 ± 15	Briant *et al.* (2006)
		LEPE03-02	X1726	146 ± 10	
		LEPE03-03	X1727	141 ± 11	
		LEPE03-04	X1728	165 ± 14	
Terrestrial deposits (terrestrial limiting)					
Pennington (overlie freshwater Ipswichian deposits)	Pennington Gravel, upper facies (FG)	PENN03-06	X1733	48 ± 5	Briant *et al.* (2006)
	Pennington Gravel, lower facies (FG)	PENN03-01	X1638	66 ± 7	Briant *et al.* (2006)
		PENN03-03	X1640	94 ± 11	

terminology; Cohen *et al.* 2022) as a value representative of mean sea-level at the peak of the sea-level transgression. The assumption is that the carving of the platform is done during transgression prior to the highstand, then at the eustatic peak of the highstand the upper shoreline angle is formed and preserved and any deposits on the terrace are then regressive. It should be noted that the global sea-level data used are a composite of various sea-level estimates, with the timing of highstands variable between reconstructions, thus multiple curves were compared to show the sensitivity of the uplift modelling to the curve chosen.

Using this uplift modelling on newly developed relative sea-level values corrected for the indicative meanings of successive sea-level indicators will give the most robust estimates of uplift rates in this region to date. Our uplift modelling shows that it is only with a significant decrease of uplift rates between the *c.* 240 or 200 and *c.* 125 ka highstands (i.e. in the Late Wolstonian and Ipswichian Stages, broadly equivalent to marine isotope stages (MIS) 7 and 5e) that the geomorphological sea-level indicators along the Sussex coast can be fitted into global sea-level curves.

Regional setting

The Solent region and Sussex coastal plain (Fig. 1) lie on the northern side of the English Channel, within the Hampshire Basin where the bedrock geology consists of Eocene and Cretaceous rocks (Melville and Freshney 1982) conducive to preserving a wide range of palaeoenvironmental indicators. Chalk forms the South Downs to the north and an east–west ridge bisecting the Isle of Wight as well as elements of the coastal plain, whereas Eocene sediments of the Lambeth, Thames, Bracklesham, Barton and Solent Groups (mainly shallow marine clays, silts and sands) rest in a series of individually subsiding basins. The two regions can be treated together structurally because all the structural features formed during the same period of compression in the Paleozoic basement rocks (Plint 1982) and are no longer active (Hopson 2009).

Modern coastal geomorphology

The present-day coast of the Solent region and Sussex coastal plain splits into three parts. In the furthest west, the Solent seaway and Southampton Water flow within poorly consolidated Eocene sediments and are flanked by low gravel cliffs of the erstwhile Solent river system (Fig. 1; e.g. Briant *et al.* 2006). Tidal range is smaller than further east, with the mean spring tidal range varying from 4.05 m in Southampton Water to 3.9 m at Calshot (east of Stone Point), 2.3 m at Lymington and 2.0 m at Hurst Point (New Forest District Council 2017). Neap tides are about half the range of spring tides. Sediment movement is dominated by estuarine and tidal flow, with some longshore drift (Fig. 2). The dominant onshore wind is from the SW.

From Portsmouth to Selsey Bill, a low coastline with three extensive harbours is cut into Eocene (Bracklesham Group) sandstones and clays (Fig. 2). A very low gravel cliff is present on both western and eastern sides of Selsey Bill, comprising sediments of the Selsey Ridge, but otherwise the area is low-lying. Offshore, bathymetric data show a series of offshore bars and banks, including the Medmerry Bank and Kirk Arrow Spit to the west (New Forest District Council 2017) and the Inner Owers to the east (New Forest District Council 2017). These banks are an important source of sediment at the present day, as are Portsmouth, Langstone and Chichester harbours, and are the ancestors of various offshore barrier systems that developed since *c.* 8000 BP, stabilizing only in 1960 (Bates *et al.* 2019). The tidal range is 4.9 m (springs) and 2.7 m (neaps) at Pagham Harbour mouth and at the entrance to Chichester Harbour, with the ebb phase shorter than the flood (New Forest District Council 2017). Offshore, most waves come from the south and SW, although the east- and west-facing coastlines on either side of Selsey Bill complicate this and parts of Bracklesham Bay (west of Selsey Bill) are partially sheltered by the Isle of Wight. Southern and eastern waves are more prevalent on the eastern side of Selsey Bill. Bracklesham Bay is therefore a swash-aligned shoreline, whereas Selsey Bill to Pagham Harbour is a drift-aligned shoreline (New Forest District Council 2017).

The third area runs from Pagham Harbour to Beachy Head (in Eastbourne) in East Sussex. This section of coast is mostly underlain by Cretaceous chalk (Fig. 1). It comprises mainly lower-lying areas with chalk cliffs of significant height developing only to the east of Brighton. River estuaries of the Arun, Adur, Ouse and Cuckmere cross the region at 90° to the coastline, but there are no natural harbours (Fig. 2). Between Brighton and Newhaven the chalk cliffs are mostly protected by coastal defences and are associated with some gravel beaches overlying shore platforms. Between Seaford Head and Beachy Head, the shore platforms are exposed chalk with scattered rocks and rock-fall sediments. The mean spring tidal range increases from west to east from 5.3 to 6.4 m. Flow is eastwards on the flood tide, westwards on the ebb (New Forest District Council 2017). The coastline is open to relatively high-energy waves from the SE, south and SW, as well as Atlantic swell waves propagating up the Channel from the west that become diffracted around the Isle of Wight. Maximum wave energy is experienced along the shoreline between Seaford and Beachy Head (New Forest District Council 2017). Beaches are dominated by gravel. Sand is sometimes present in the foreshore, but not where shoreline platforms occupy most of the inter-tidal zone. The dominant transport of coarse sediment is west to east (New Forest District Council 2017; Fig. 2).

Pleistocene sea-level indicators

During the Pleistocene the region was dominated by two major geomorphological systems consisting of the Solent River system to the west draining large parts of the Hampshire Basin (Allen and Gibbard 1993; Briant *et al.* 2006; Westaway *et al.* 2006) and the English Channel or Manche coastline to the east (Bates *et al.* 2003). Transformation of a Manche embayment into an open seaway during the Middle Pleistocene (Gibbard 1988, 1995) allowed transfer of marine waters from the southern North Sea into the English Channel from the Anglian or Elsterian Stage onwards during periods of sea-level highstand. This occurred as a result of overflow of an ice-dammed lake and was completed during a second phase of lake formation at the very end of the Wolstonian or Saalian Stage (Gupta *et al.* 2007; Busschers *et al.* 2008). A number of palaeo-sea-level indicators are preserved in the area. These are described below, using the categories in the WALIS database (Cohen *et al.* 2022).

The chronostratigraphic sequence of the British Isles (Bowen 1999) identifies only one stage (the Wolstonian Stage) between the Hoxnian and Ipswichian Stage interglacials. However, it has been shown, through a dual process of biostratigraphic refinement and comparison of terrestrial records with the more complete global marine record, that it is likely that the Wolstonian Stage encompasses multiple climatic cycles. Because this scheme does not have enough formally specified stages to capture all of the complexity now recognized in the British terrestrial record, previous reserchers have sought to establish the age of sea-level highstand sequences in the Sussex coastal plain by direct reference to marine isotope stages. This can be problematic, because the global ice volume changes recognized in the composite marine stratigraphy do not correspond directly to terrestrial climatic events, particularly because the signal is dominated by the Laurentide ice sheet, which does not seem to have expanded in synchronicity with ice sheets in the British Isles and NW Europe (Gibbard and Hughes 2021). It is less problematic for sea-level than ice volume changes, because this

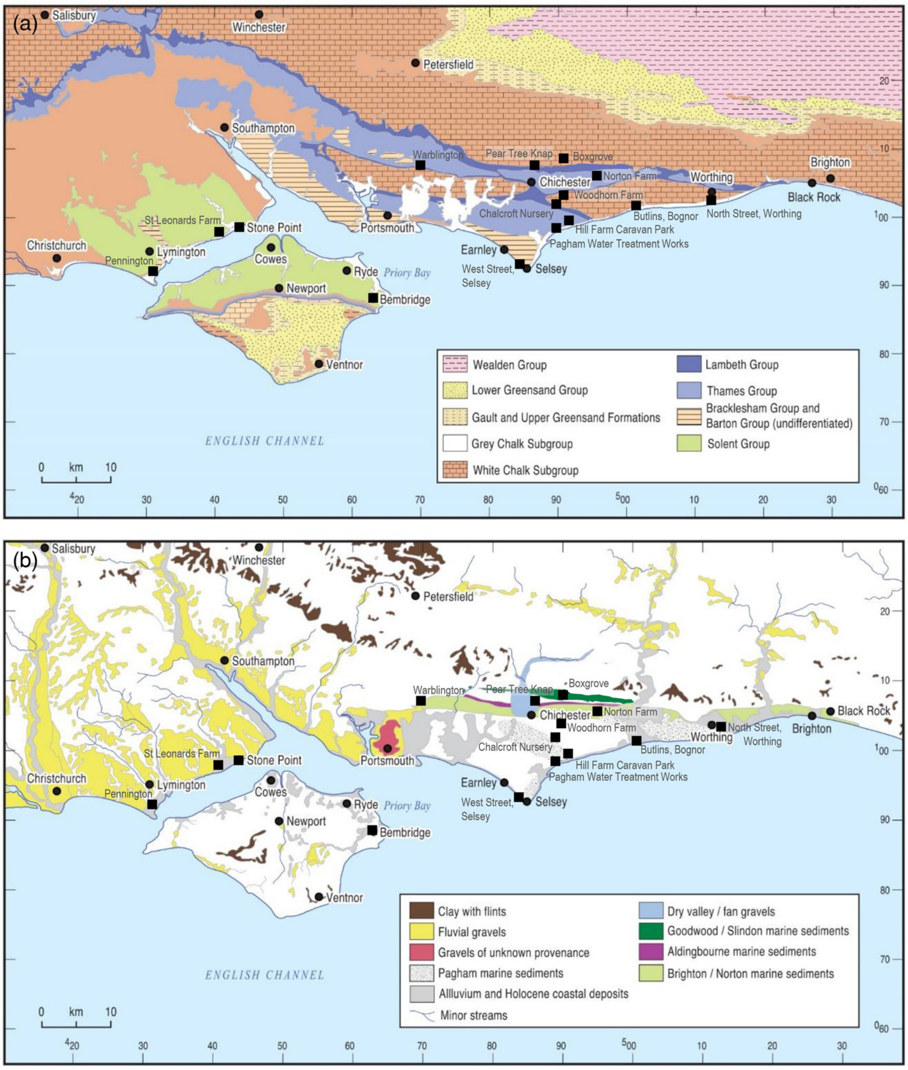

Fig. 1. Map of the Solent region and Sussex coast, showing location of sites mentioned in the text, Figures 3–6 and Tables 1–4.

signal is more globally synchronized, but even these have some regional variability. Therefore, in this paper we primarily apply a terrestrial stratigraphy using the newly suggested subdivision of the Wolstonian Stage into Early, Middle and Late Substages (Gibson *et al.* 2022). The Early Wolstonian Substage comprises a glacial period immediately following the Hoxnian interglacial, whereas the Middle and Late Wolstonian Substages each encompass a full climatic cycle (both glacial and interglacial). Where appropriate, to aid comparison with work by previous researchers, dated highstand events are noted, as is likely equivalence to marine isotope stages.

Marine terraces

The oldest marine terrace feature is developed in Cretaceous chalk and underlies deposits of the Goodwood–Slindon Formation (Fig. 1). It is best developed at Boxgrove, where the inner margin of the marine terrace has a value of 39 ± 1.5 m OD (Ordnance Datum; i.e. mean sea-level) (Figs 3b and 4, Table 2). This is overlain by successively finer deposits, which were laid down in a back-barrier setting (Roberts and Parfitt 1999) with a total sequence thickness of 10–15 m. These deposits are argued to date from the end of the Cromerian Stage, equivalent to MIS 13 (i.e. 478–524 ka) on the basis of biostratigraphy (Roberts and Parfitt 1999). They probably relate to the *c.* 485 ka highstand seen in multiple global sea-level compilations (e.g. Grant *et al.* 2014). The coastline during deposition of this Formation and prior to the formation of the Straits of Dover was a sheltered embayment (Bates *et al.* 2010).

A further lower marine terrace is also developed within the Cretaceous chalk. This is overlain by beach gravels, some beach sands and several metres of clay-rich solifluction deposits. The two best exposures of this sequence of deposits, termed the Brighton–Norton Formation (Fig. 3b), are at Norton Farm (Figs 1 and 4; Bates *et al.* 2010) and Black Rock, Brighton (Briant *et al.* 2022), but only at Norton Farm are there elevation measurements or age estimates. At Norton Farm, the inner edge of the marine terrace has a value of 7.2 ± 1.5 m OD (Table 3), formed in Cretaceous chalk, but showing a transition to sands and clays of the Lambeth and Thames Groups within 50 m offshore. Microfossils suggest that the sands are marine and include cold-water indicators (Bates *et al.* 2010) that are overlain by regressive units (Fig. 3). The overlying silts are terrestrial, being rich in freshwater molluscs. The OSL age from the borehole closest to the inner edge (BH16) is 238 ± 27 ka, at the start of the Late Wolstonian Substage. It was attributed to the earlier part of MIS 7 by Bates *et al.* (2010), which might suggest deposition during the *c.* 240 ka global highstand (Grant *et al.* 2014). Alternatively, the cold-water microfossils and the small horse and mammoth fauna found at Westhampnett, Norton Farm and Black Rock (Bates *et al.* 2010), suggesting late interglacial conditions, possibly relate to the global highstand at *c.* 200 ka. This later highstand, however, has approximately the same elevation as the 240 ka highstand relative to today (e.g. Bates *et al.* 2014; Grant *et al.* 2014). The Brighton–Norton Formation is the earliest evidence for a more open coastline in the region (Fig. 1; Bates *et al.* 2010).

Fig. 2. Geomorphological setting of the Solent region and Sussex coast showing offshore bathymetry from the South East Regional Coastal Monitoring Programme, available under Open Government License version 3 (Channel Coast Observatory, 2021), dominant sediment movements from New Forest District Council (2017) and the modern analogue locations used to calculate indicative meanings for relative sea-level estimates.

A marine terrace is also formed further west within the more erodible Bembridge Limestone at Bembridge on the Isle of Wight (Fig. 1). The exact location of the inner edge is less clear because the angle of the former cliff is less steep than those formed in chalk but is measured to *c.* 6 ± 2 m OD (Fig. 5). The terrace is overlain by a thick sequence of marine gravels rising to 18 m OD (Tables 2–4, Figs 3 and 5; Preece *et al.* 1990). Sand and gravel near, but not directly overlying, the inner edge of this marine terrace were dated to the Ipswichian Stage; that is, the *c.* 125 ka highstand (Table 2; Wenban-Smith *et al.* 2005).

Beach deposit and beach rock

Beach gravels attributed to the Aldingbourne Formation (intermediate in elevation between the Goodwood–Slindon and Brighton–Norton formations; Fig. 1b) are the youngest sediments associated with the 'embayed coastline phase' identified by Bates *et al.* (2010) and included in the WALIS database (Table 1). Where investigated, the base of these deposits is found at *c.* 18–20 m OD (Bates *et al.* 2010). The thickness of these deposits is *c.* 3 m. Despite their position on the edge of the chalk, they are mostly decalcified, making palaeoenvironmental interpretations and biostratigraphic age assignment hard. It is possible that these deposits are of mixed age because a variety of marine, brackish, freshwater and terrestrial sequences have been recovered between Fontwell and Tangmere. The Aldingbourne Formation deposits fall within the Wolstonian Stage. They were assigned to MIS 7 or Late Wolstonian Substage by Bates *et al.* (2010) on the basis of OSL ages ranging from 182 to 265 ka from Norton Farm and younger OSL ages from Pear Tree Knap of *c.* 90–190 ka, thought to be too young because of the altitude of these deposits and the saturation of the signal (Bates *et al.* 2010). It should be noted that *c.* 250 ka is close to the age at which quartz OSL signals saturate at the relatively low dose rates common in England (Rixhon *et al.* 2017).

The lowest elevation palaeo-sea-level indicators (Table 1) in the Sussex coastal plain (Pagham Formation) are also beach deposits, occurring closest to the present-day coastline (Fig. 1b), located between Chichester and Worthing, and typically, but not exclusively, with lowest contacts below 5 m OD (Fig. 3). These sequences are not associated with a preserved marine terrace and occur at a range of altitudes. They comprise both gravels and sands and contain well-preserved and diverse ostracod and foraminifera assemblages. These marine sequences are assigned to the Ipswichian Stage on the basis of OSL dating (Table 3, Fig. 3a). The most distinctive deposit of this type is the Selsey Ridge (Bates *et al.* 2009*a*). This is a ridge of sand and rounded gravels currently exposed at the coast at Selsey Bill and forming a low cliff (*c.* 5 m OD top surface) where the deposits are truncated by the modern coastline (Fig. 2a). The ridge has been interpreted as an offshore bar

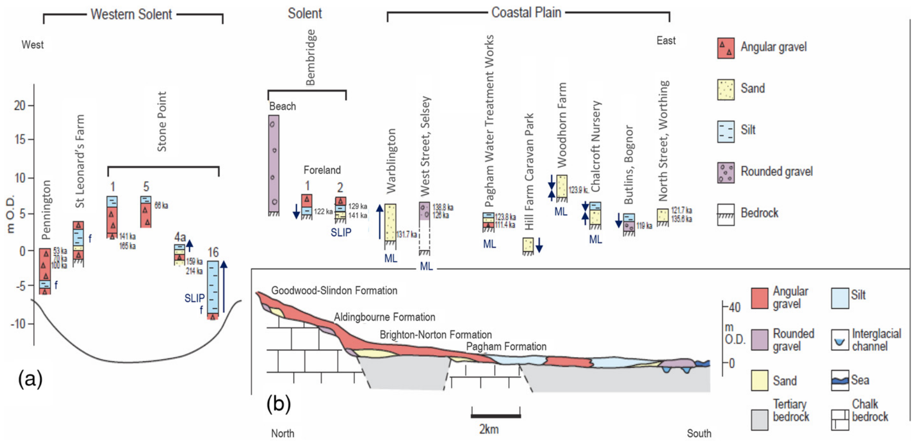

Fig. 3. (**a**) Lithological profiles and optically stimulated luminescence (OSL) dates (see also Table 3) through selected MIS 5e sites from the Solent region and the Sussex coast. ML, sites used as marine limiting data; SLIP, sites used as sea-level index points, both in the WALIS database. f, freshwater sequence; ↑, transgressive sequence (contains reworked warm elements and foram *Ammonia batavus* (ornate)); ↓, regressive sequence (contains shallow-water foram species *Elphidium williamsonii* and freshwater ostracods). (**b**) Schematic profile through raised marine sediments of the Sussex Hampshire Coastal Corridor, showing which groups of sediments are associated with marine terraces. Sources: (a) WALIS database, Cohen *et al.* (2022). Sequences have been described fully by Allen *et al.* (1996), Wenban-Smith *et al.* (2005), Briant *et al.* (2006, 2013, 2022) and Bates *et al.* (2010) or are previously unpublished (Butlins, Bognor and North Street, Worthing; Supplementary material Table S1).

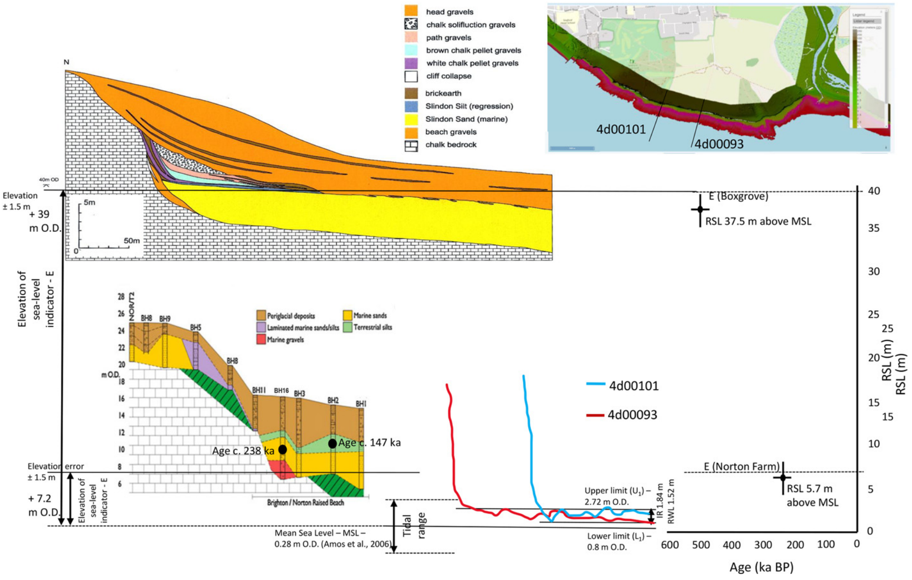

Fig. 4. Calculation of indicative sea-level meaning of the raised clifflines at Boxgrove and Norton Farm, using the methodology of Rovere *et al.* (2016). The Boxgrove sequence shown is from Quarry 2 (figure 31, Briant *et al.* 2022) and the Norton Farm sequence is shown in figure 6 of Bates *et al.* (2010). The modern analogue of a cliffline developed in Cretaceous Chalk is Seaford Head (location c on Figure 2). The 2018 LIDAR profiles across Seaford Head and bathymetry shown come from the South East Regional Coastal Monitoring Programme, available under Open Government License version 3 (Channel Coast Observatory, 2021).

by Bates *et al.* (2010). This is the most exposed part of the Solent estuary with the greatest fetch from the Channel, so the development of such bars would be expected at this location, as is seen in the modern coastal system (Fig. 2). Although none of the ostracod and foraminifera assemblages yield evidence of specific water depths, some show transgression; for example, at the Pagham Water Treatment Works where small numbers of *Elphidium williamsonii* at the base of the sequence are replaced upwards by an ornate form of *A. batavus* argued by Bates *et al.* (2010) to be indicative of high-energy environments, as would be likely during transgression. In addition, some sequences show regression; for example, in parts of the sequences at Warblington, Woodhorn Farm, Mill Farm Caravan Park and North Street, Worthing. Regression here is suggested by elements suggesting colder water conditions; for example, *Cassidulina reniformis* and *Elphidium clavatum* at Warblington and Woodhorn Farm and dwarfed versions of *A.* batavus and *Elphidium fichtellianum* at Warblington, Woodhorn Farm and at Mill Farm Caravan Park (Bates *et al.* 2010). The regressive or transgressive tendencies are shown in Figure 3 and all these sites were included in the WALIS database (Table 1). The sequences of the Pagham Formation were interpreted by Bates *et al.* (2010) to represent a harboured coastline phase where the offshore bar of the Selsey Ridge formed a protected coastal plain behind which shallow 'harbours' developed despite the full opening of the Straits of Dover by this time (Busschers *et al.* 2008).

Salt marsh and estuary deposits

An estuarine sequence of Ipswichian age, also listed in the WALIS database (Table 1), is preserved at Stone Point (Fig. 1), originally studied by West and Sparks (1960), Brown *et al.* (1975) and Briant *et al.* (2009). Briant *et al.* (2019) extended the interglacial sequence to −9 m OD (borehole 16, Fig. 3a). Their unit 2 records the transition from freshwater (units 2a to 2c) to estuarine deposits (unit 2d). This latter is a stiff grey clay with shells, interbedded with thin discontinuous beds of compressed wood-peat, especially in the upper parts of the profile and extending in depth from −8.5 to 1 m OD (Briant *et al.* 2019). The pollen from unit 2d suggests mixed-oak woodland (Ipswichian pollen zone Ip IIa grading upwards into Ip IIb). The estuarine deposits grade upstream into silts at the nearby site of Pennington Marshes (*c.* 17 km upstream). Here, Ipswichian Stage deposits with freshwater affinities occur at −3.9 to −5.3 m OD depth and yield pollen suggestive of a transition from the pre-temperate (Ip I) to early temperate (Ip II) zones (Allen *et al.* 1996).

In addition, at St Leonards Farm *c.* 5 km upstream of Stone Point, decalcification and poor fossil preservation means that silts from *c.* 0.1 to 1.8 m OD cannot be attributed to either freshwater or estuarine deposits. The pollen records a transition from oak-dominated assemblages typical of the early temperate zone (Ip II) to a birch–pine–alder assemblage that may be late temperate (Ip III), although pollen preservation in this part of the sequence is very low (Briant *et al.* 2013).

Further saltmarsh deposits are preserved on the Isle of Wight. Somewhat enigmatic and truncated deposits of the Steyne Wood Clay occur at *c.* 40 m elevation and may be coeval with the Goodwood–Slindon Formation (Briant *et al.* 2022). A more complete sequence is associated with the lower Bembridge marine terrace. Here at Bembridge Foreland is an Ipswichian age saltmarsh sequence used as a sea-level index point in the WALIS database (Table 1, Fig. 3). At the top of this sequence (Table 4), pollen records document saltmarsh conditions giving way to freshwater marsh up-profile, a locally regressive trend during the early to late temperate vegetation transition (Ip II–III). These fossil-bearing deposits are at *c.* 5–6 m OD, overlying the thinner, northeastern end of the thick sequence of gravels overlying the marine terrace (Preece *et al.* 1990; Wenban-Smith *et al.* 2005).

Materials and methods

Field description and sampling

The sequences studied were retrieved from a mixture of open sections, test pits and boreholes. Field description and sampling were followed by sieving and analysis of fossils, using methods described by Bates *et al.* (2004). Where fossils were previously published, the original references are cited in the text. Supplementary material Table S1 contains fossil data from sites that have not previously been published.

Geochronology

Age control on MIS 5e deposits from the Solent and Sussex coastal plain is provided primarily by OSL (Wenban-Smith *et al.* 2005; Briant *et al.* 2006; Bates *et al.* 2010) (Table 2, Figs 2 and 3). Amino acid racemization was less successful because of the lack of freshwater molluscs for analysis (Bates *et al.* 2004; Briant *et al.* 2006). Dating is based on both direct dating of marine sands and indirect dating of bracketing cold stage fluvial deposits (Table 2).

Table 3. Indicative meaning of palaeo-sea-level indicators at Boxgrove, Norton Farm, Bembridge and various sites within the Pagham Formation on the Sussex coastal plain, using modern analogues at Seaford Head, Hamstead Cliffs and Selsey Bill and the method of Rovere et al. (2016)

	Elevation (m)	Error (m)	Reference water level (RWL) (m)	Indicative range (IR) (m)	Relative sea-level (RSL) (m)	Error (δRSL) (m)	Comments on sequence
Marine terraces, elevation of inner edge of shore platform							
Boxgrove (Goodwood–Slindon Formation)	39	1.5	1.52	1.84	37.5	1.7	
Norton Farm (Brighton–Norton Formation)	7.2	1.5	1.52	1.84	5.7	1.8	
Bembridge (Ipswichian age, equivalent to Pagham Formation)	6	2	0.71	0.89	5.3	2	
Beach deposits, elevation of top of deposit within Pagham Formation							
West Street Selsey	7	1	1.73	7.74	5.3	4.0	Not truncated
Warblington	7	2	1.73	7.74	5.3	4.4	Not clear if truncated
Chalcroft Nurseries	6	1	1.73	7.74	4.3	4.0	Overlain by silt; probably not truncated
Pagham Water Treatment Works	4.8	1	1.73	7.74	3.1	4.0	Overlain by silt; probably not truncated
Woodhorn Farm	11	2	1.73	7.74	9.3	4.4	Not clear if truncated
Butlins Bognor	4.5	2	1.73	7.74	2.8	4.4	Not clear if truncated
North Street Worthing	6	2	1.73	7.74	4.3	4.4	Not clear if truncated
Mill Farm Caravan Park	2	2	1.73	7.74	0.3	4.4	Not clear if truncated

U_1 (L_1), upper (lower) range of landform in modern analogue in relation to mean sea-level; IR, indicative range = U_1-L_1; RWL, reference water level = $(U_1 + L_1)/2$; E, elevation of palaeo-sea-level indicator above MSL, with error (E_e); RSL, palaeo-relative sea-level = E-RWL; δRSL, error on RSL = Sqrt $((IR/2)^2 + (E_e/2)^2)$. Modern analogues are shown in Figures 4–6 and locations are shown in Figure 2.

Table 4. Details of the Bembridge Foreland sequence, Isle of Wight

Southwestern sedimentary sequence (palaeocliffline) and elevation	Interpretation	Chronological control	Northeastern sedimentary sequence (Bembridge Foreland) and elevation
Brickearth up to 10 m thick adjacent to palaeocliffline, 15–27 m OD	Possibly aeolian	TL *c.* 18 and 24 ka (Parks and Rendell 1992)	Thin brickearth, above Bembridge Foreland pollen sequence, *c.* 7–8 m OD
Thin layer of clayey gravel, *c.* 18 m OD	Colluvial or solifluction	OSL 1,2, 8, *c.* 82, 103 and 116 ka (Wenban-Smith *et al.* 2005)	Thick layer of clayey gravel, with some sand at base, *c.* 6–7 m OD
	Salt marsh sediments adjacent to main beach (Preece *et al.* 1990), freshening upwards (Wenban-Smith *et al.* 2005)	OSL 4, *c.* 129 ka (Wenban-Smith *et al.* 2005); early to late temperate pollen assemblages	Bembridge Foreland pollen sequence: pollen-bearing humic silt *c.* 5–6 m OD
	Estuarine sediments	OSL 5 and 6, *c.* 141 and 157 ka (Wenban-Smith *et al.* 2005)	Clay–silt, fine sand, *c.* 4–5 m OD
Sand and gravel, *c.* 4–18 m OD, next to palaeocliffline	Cuspate foreland storm beach (Preece *et al.* 1990)	TL *c.* 104 and 115 ka (Preece *et al.* 1990, appendix B); OSL 3 and 7, *c.* 122 and 183 ka (Wenban-Smith *et al.* 2005)	Sand and gravel, *c.* 4–5 m OD

Descriptions are a summary of work presented by Preece *et al.* (1990) and Wenban-Smith *et al.* (2005). Full OSL age details for key samples are given in Table 2.

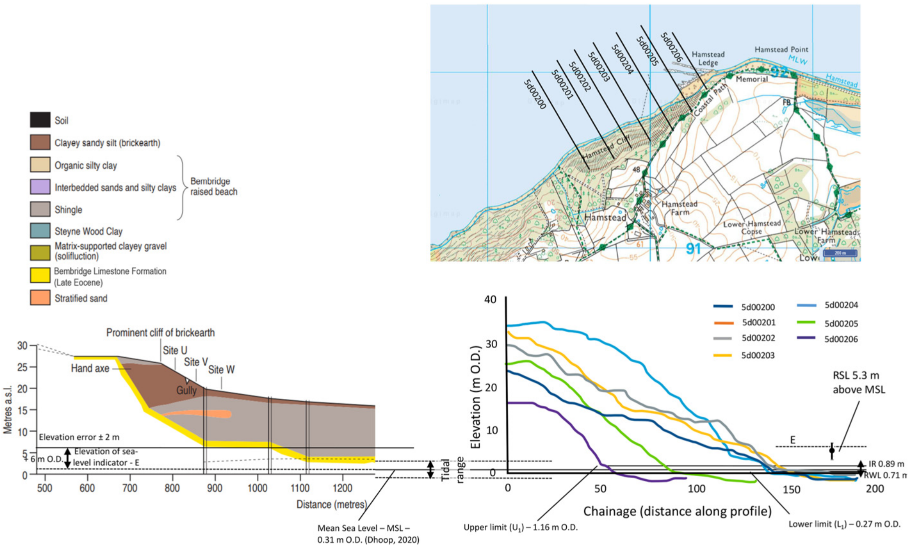

Fig. 5. Calculation of indicative sea-level meaning of the raised cliffline at Bembridge. The modern analogue used is a cliffline developed in Bembridge Limestone is Hamstead Cliffs (location a in Fig. 2). Sources: calculation uses method of Rovere *et al.* (2016). The Bembridge sequence shown is from figure 12 of Briant *et al.* (2022). The 2008 LiDAR profiles across Hamstead Cliffs come from data available from the Channel Coast Observatory (2021). Ordnance Survey mapping used under Digimap license to Birkbeck University of London.

Determining indicative meaning from palaeo-sea-level indicators

A robust way of assessing how palaeo-sea-level indicators relate to past mean sea-levels is to use the indicative meaning approach of Rovere *et al.* (2016). This approach takes into account the exact local relationships between modern analogues for a preserved geological sea-level indicator and mean sea-level; for example, is the inner edge of a marine terrace formed at the present-day mean sea-level or instead formed above or below? This is called the reference water level (RWL) for this feature and the error on this estimate is the indicative range (IR). The relative sea-level (RSL) and associated error (δRSL) are then estimated by adjusting measured present-day elevations of features using the RWL and IR. Indicative meanings were calculated both for marine terraces for use in uplift modelling and also for Pagham Formation beach deposits to compare with the estimate from Kopp *et al.* (2009). The features used to determine palaeo-RSL values are different from those used by Cohen *et al.* (2022), who calculated these only for beach deposits of the Aldingbourne Formation and the saltmarsh sequences at Bembridge and Stone Point (Table 1).

The modern analogue used to assess the indicative meaning of the two modelling tie-points at Boxgrove and Norton Farm comes from Seaford Head, which is the closest marine terrace to the sites that was developed in Cretaceous chalk and not directly affected by coastal protection structures (Fig. 2). Several LiDAR profiles to the east of Seaford Head were used to assess the upper and lower limits of the inner edge of the modern marine terrace. These were chosen on the basis of completeness of data and clarity of the junction between the cliff face and the marine terrace. The final values used are an average value from all the cliff profiles used (Fig. 4) and the adjusted relative sea-level shown in Table 3.

The modern analogue used to assess the indicative meaning of the modelling tie-point at Bembridge comes from Hamstead cliffs on the NE coast of the Isle of Wight near Yarmouth because the Bembridge Limestone is obscured by the Pleistocene sequence at Bembridge itself and other locations have significant beach thicknesses. Even here, the Bembridge Limestone is exposed only at the base of the cliff (Gale 2019). However, because the transition to the overlying Hamstead Member is above the cliff–terrace junction, the inner edge of the marine terrace is still adequately preserved in Bembridge Limestone. LiDAR profiles along the full length of the cliffs were used to assess the maximum and minimum levels of the inner edge of the modern marine terrace. The final values used are an average value from all the cliff profiles used (Fig. 5) and the adjusted relative sea-level shown in Table 3.

Indicative meanings of the beach deposits from the Pagham Formation can be calculated but are known less precisely because of

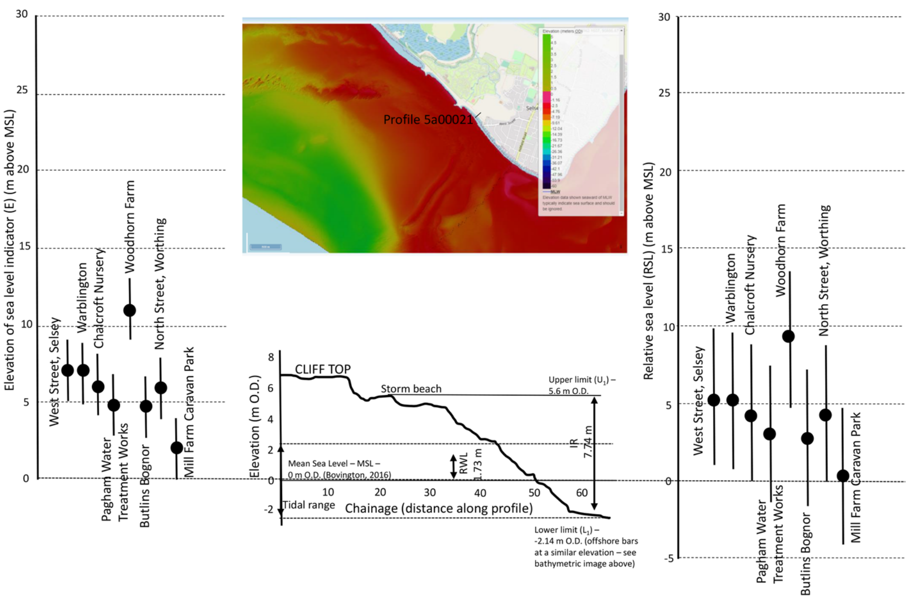

Fig. 6. Calculation of indicative sea-level meaning of the Pagham Formation marine sediment sequences on the West Sussex coastal plain as shown on Figure 3, using the methodology of Rovere *et al.* (2016). The modern analogue used is Selsey Bill (location b on Figure 2). The beach profile across Selsey Bill and the bathymetry shown come from the South East Regional Coastal Monitoring Programme, available under Open Government License version 3 (Channel Coast Observatory 2021).

the lack of a marine terrace and because beach elevations vary significantly seasonally. In addition, modern coastal deposits use the top of the deposit as an elevation tie-point, but the elevation of the top of the palaeo-sea-level indicators is not necessarily comparable because the deposit may have been truncated since deposition. To address this issue, larger error bars were given where the Pagham Formation deposits were visibly truncated (3 m), smaller where they were visibly not truncated (1 m) and intermediate otherwise (2 m). The modern analogue used here was a beach profile from West Street Selsey, qualitatively sense-checked by comparison with bathymetric data shown in Figure 2 to assess the relative elevation of offshore banks and bars. The final elevations used incorporate a significant error (Fig. 6) and the adjusted relative sea-levels are given in Table 3.

Synchronous correlation uplift modelling

Where age controls are available within a marine terrace sequence, the synchronous correlation approach tests whether the elevations of undated marine terraces can be explained by the uplift rates implied by the elevations of dated marine terraces. In doing so, synchronous correlation can be used to 'predict' the elevations of marine terraces that may not be observable in the landscape. The non-linear temporal spacing of sea-level highstands results in marine terraces and their associated marine terraces that are not evenly spaced in elevation (Houghton *et al.* 2003; Roberts *et al.* 2009; Grant *et al.* 2014). Indeed, highstand variation over time combined with tectonic uplift may result in the destruction of older marine terraces by younger marine highstands, particularly, as here, where uplift rates are low (e.g. Westaway *et al.* 2006; Roberts *et al.* 2009; Pedoja *et al.* 2014, 2018; Jara-Muñoz and Melnick 2015; Normand *et al.* 2019). The synchronous correlation method therefore recognizes that not all marine terraces in a profile will sequentially represent all sea-level highstands (e.g. Robertson *et al.* 2019; De Santis *et al.* 2023).

Specifically, the synchronous correlation approach uses dated marine terraces as 'tie-points' to constrain the uplift rate at the highstand associated with the age control (e.g. Roberts *et al.* 2009). Initially, these absolute age constraints are used to drive the simplest hypothesis of a constant uplift rate through time, but more complex uplift scenarios are tested if a constant uplift rate cannot be successfully applied to explain the marine terrace elevations within the entire sequence.

The tie-points used in this study were the adjusted relative sea-levels shown in Table 3 associated with marine terrace inner edges at 37.5 ± 1.7 m OD at Boxgrove for the 485 ka highstand (Roberts and Parfitt 1999) and 5.3 ± 2 m OD at Bembridge at the 125 ka highstand (Preece *et al.* 1990; Wenban-Smith *et al.* 2005). The tie-point at Norton Farm of 5.7 ± 1.8 m OD was not used because of the uncertainty over which highstand (200 or 240 ka) it related to. The uplift rates were iterated until the predicted marine terrace elevations matched those associated with the observed, dated marine terraces. The resultant uplift rate was applied to the marine terrace inner edge sequence, the outcome of which is a set of predicted marine terrace elevations that were matched to elevation observations to allow correlation between undated marine terrace inner edges and sea-level highstands. Herein, we use eustatic sea-level highstand timing and elevation data from Grant *et al.* (2014), as these give the global sea-level curve that shows the most detail (Table 5).

It has been shown that different late Quaternary sea-level curves reveal variations in the timing and elevations of past sea-level highstands, which may affect highstand to marine terrace inner edge correlations and uplift rate determinations (e.g. Caputo 2007; Robertson *et al.* 2019; De Gelder *et al.* 2020). Consequently, we also tested how the results of our synchronous modelling using the sea-level data of Grant *et al.* (2014) varied when sea-level curves of Bintanja *et al.* (2005), Bates *et al.* (2014) and Spratt and Lisiecki (2016) were employed. These sea-level curves were selected as representative of a range of possible values because they extend back to the assumed age of the Boxgrove tie-point and have been constructed using differing approaches (i.e. hydraulic modelling, Grant *et al.* (2014); principal component statistical analyses using numerous sea-level datasets, Spratt and Lisiecki (2016); ice-sheet–ocean temperature models from oxygen isotope ratios in benthic foraminifera, Bintanja *et al.* (2005); transfer functions associated with 10 marine sediment cores, Bates *et al.* (2014)).

Results

Indicative meanings and relative sea-level estimates

Figures 4–6 and Table 3 show the relative sea-levels of the three marine terraces in the region at Boxgrove, Norton Farm and Bembridge and the various Ipswichian Stage beach deposits of the Pagham Formation. Comparing Figures 4 and 5 with Figure 6, it is clear that it is possible to estimate indicative meaning more precisely for marine terraces (1.84 m indicative range at Seaford Head and 0.89 m at Hamstead) than for beach deposits (7.74 m indicative range). This is because it is not possible to say from the beach sequences preserved what type of beach is represented, nor how far inland or offshore it is. It is probably for this reason that Cohen *et al.* (2022) listed these as marine limiting datapoints (Table 1) rather than sea-level indicators. In all cases, the reference level is above mean sea-level, meaning that the relative sea-level estimate from the sites is lower in elevation than the actual feature.

Synchronous correlation uplift modelling

Given the uncertainty over the age of the Norton Farm tie-point, initial uplift rate iterations used only the two tie-points with indicative meanings of 37.5 m (Boxgrove, 485 ka) and 5.3 m (Bembridge, 125 ka). It proved impossible to fit these tie-points with a single uplift rate, but a rate change between the 200 and 125 ka highstands allowed all dated tie-points to be correctly placed (Fig. 7, Table 5). This model solution suggests that the Norton Farm tie-point is more likely to relate to the 240 ka highstand in the Late Wolstonian Substage (*c.* MIS 7e) and that the Aldingbourne Formation may date from the 335 ka highstand in the Middle Wolstonian Substage (*c.* MIS 9). The former agrees with OSL dating but not biostratigraphy, and the latter conflicts with published OSL dating although not unpublished data (see discussion below). The latter is older than multiple adjacent OSL ages deemed to be reliable by Bates *et al.* (2010) and requires further investigation. An uplift rate change at 140 ka fits the data best. This is approximately coeval with a sea-level lowstand adjacent to Termination 2 in the marine record (Lisiecki and Raymo 2005), also termed the 'Penultimate Glacial Maximum' (Gibbard and Hughes 2021). Using Grant *et al.* (2014) models, until *c.* 140 ka the uplift rate was *c.* 0.164 mm a^{-1} reducing to 0.005 mm a^{-1} from *c.* 140 ka to the present day with a propagated error of 0.13 mm a^{-1}. It is possible, however, that this change occurred gradually between the 240 and 125 ka highstands rather than at a single point in time, or closer to *c.* 160 ka when ice extents in NW Europe were at their maximum during the Moreton and Drenthe Stadials (Gibbard *et al.* 2022; Gibson *et al.* 2022). Although a 160 ka rate change results in an acceptable fit between the measured and predicted elevations in our modelling within its uncertainties, we prefer to employ a rate change at 140 ka because we observe a better match between the measured elevations and those predicted in the modelling. The uncertainties are high compared with the uplift rates themselves but this is an inevitable function of the errors on global sea-level curves, which can be of the order of *c.* 12 m (e.g. Siddall *et al.* 2003; Bintanja *et al.*

Table 5. Best-fit modelling results for Grant et al. (2014) and various comparator sea-level curves chosen to represent different types of reconstruction

British Stage or Substage		NW European Stage	Equivalent marine isotope stage (MIS)	Sussex marine terrace tie-points	Grant *et al.* (2014) 0.164 mm a^{-1} 485–140 ka; 0.005 mm a^{-1} 140 ka to present		Spratt and Lisiecki (2016) 0.13 mm a^{-1} 485–140 ka; 0.015 mm a^{-1} 140 ka to present		Bintanja *et al.* (2005) 0.164 mm a^{-1} 485–140 ka; 0.005 mm a^{-1} 140 ka to present		Bates *et al.* (2014) 0.164 mm a^{-1} 485–140 ka; 0.005 mm a^{-1} 140 ka to present	
				Corrected relative sea-level (m)	Highstand date	Predicted back point elevation (m)	Highstand date	Predicted back point elevation (m)	Highstand date	Predicted back point elevation (m)	Highstand date	Predicted back point elevation (m)
Devensian		Weichselian	MIS 5d-2		37000	−72.0						
					58000	−65.2	53000	−61.2	50000	−77.5	55000	−50.0
					84875	−34.8	82000	−25.8	80000	−34.6	80000	−12.0
					106500	−30.0	102000	−14.5	98000	−31.1	100000	−8.0
Ipswichian		Eemian	MIS 5e	Pagham , Bembridge beach: 5.3 ± 2	127750	5.3	120000	5.8	123000	5.7	125000	8.0
Wolstonian	Late	Saalian	MIS 6		171500	−50.6	168000	−49.3	172000	−65.0	175000	−44.8
			MIS 7d-a		196875	−2.0	198000	−2.4	198000	−6.2	200000	−2.9
					213900	−15.4	225000	4.2	215000	−2.2	210000	−1.7
			MIS 7e	Brighton–Norton Fm:5.7 ± 1.8	239750	5.5	236000	4.6	238000	4.0	240000	6.9
	Middle		MIS 8		258875	−54.2						
					291750	−11.1	284000	−13.2	285000	−8.4	280000	4.7
			MIS 9	Aldingbrn Fm?	315375	−8.2			307000	14.6		
	Early		MIS 10		328000	21.1	330000	23.8	340000	45.6	325000	24.0
			MIS 11b		350000	−54.8	383000	13.7				
Hoxnian		Holsteinian	MIS 11c		405625	38.2	404000	46.4	410000	53.3	410000	34.1
Anglian		Elsterian	MIS 12		442375	−54.9						
Cromerian		'Cromerian complex' Interglacial IV	MIS 13	Goodwood–Slindon Formation: 37.5 ± 1.7	485000	38.2	485000	37.0	488000	37.5	495000	37.2

Types of reconstruction: hydraulic modelling, Grant *et al.* (2014); principal component statistical analyses using numerous sea-level datasets, Spratt and Lisiecki (2016); ice-sheet–ocean temperature models from oxygen isotope ratios in benthic foraminifera, Bintanja *et al.* (2005); transfer functions associated with 10 marine sediment cores, Bates *et al.* (2014). Stratigraphic comparisons follow the schemes of Gibbard and Hughes (2021) and Gibson *et al.* (2022).

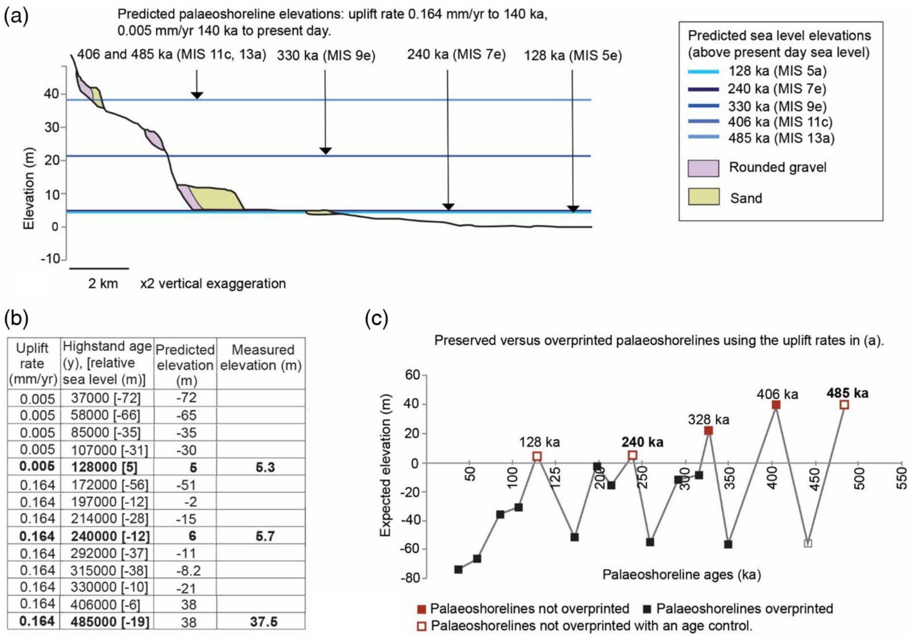

Uplift rate (mm/yr)	Highstand age (y), [relative sea level (m)]	Predicted elevation (m)	Measured elevation (m)
0.005	37000 [-72]	-72	
0.005	58000 [-66]	-65	
0.005	85000 [-35]	-35	
0.005	107000 [-31]	-30	
0.005	**128000 [5]**	**5**	**5.3**
0.164	172000 [-56]	-51	
0.164	197000 [-12]	-2	
0.164	214000 [-28]	-15	
0.164	**240000 [-12]**	**6**	**5.7**
0.164	292000 [-37]	-11	
0.164	315000 [-38]	-8.2	
0.164	330000 [-10]	-21	
0.164	406000 [-6]	38	
0.164	**485000 [-19]**	38	**37.5**

Fig. 7. Synchronous correlation modelling results. (a) Topographic profile across the Sussex coastal plain with measured palaeoshorelines matched to highstand elevations predicted by the Terrace Calculator as described in the text. (b) Table of predicted uplift rates and shoreline elevations from Grant *et al.* (2014). (c) Graphical representation of expected elevations of global sea-level highstands using the uplift rates in (a) showing which will be preserved and which overprinted.

2005; Grant *et al.* 2014; Rohling *et al.* 2014). However, we note that the sea-level elevations close to or above present day may be better defined (e.g. those at MIS 1, 5e, 9e and 1c; Past Interglacials Working Group of PAGES 2016). We also note that similar propagated errors occurred in the study by Pedoja *et al.* (2018) of slow coastal uplift on the Cotentin Peninsula, France.

Comparing the outcome of using different sets of sea-level curve data in our uplift modelling (Bintanja *et al.* 2005; Bates *et al.* 2014; Spratt and Lisiecki 2016) with the results using Grant *et al.* (2014) shows a similar temporal pattern, although different values (Table 5). This is because in many of these reconstructions a younger highstand has a sea-level elevation higher than the 485 ka highstand, which would mean that the 485 ka highstand is destroyed by that at 340 ka or 410 ka, for instance. However, it would be extremely surprising if the exact uplift rates were the same given the different datasets on which the various sea-level curves are based. Table 5 clearly shows that a similar temporal pattern is maintained regardless of which sea-level curve is used, in which the rate from 485 to 140 ka is between 0.07 and 0.2 mm a^{-1}, dropping after 140 ka to 0–0.005 mm a^{-1} (with the exception of the rate of Spratt and Lisiecki 2016, which drops to 0.1 mm a^{-1}).

Discussion

Refining relative sea-level estimates for the Sussex coastal plain using indicative meanings from modern analogues

This study has produced three new detailed palaeo-RSLs for marine terraces based on modern analogues (Table 3). These are reliable geomorphological landforms because they have the narrowest elevation range in relation to mean sea-level in the modern coastal setting. They are also the geomorphological indicators for which the synchronous correlation modelling approach has been developed. The use of modern analogues was the preferred approach of Rovere *et al.* (2016) for determining palaeo-RSLs. All these palaeo-RSL values have been estimated at lower elevations (37.5 m at Boxgrove, 5.7 m at Norton Farm and 5.3 m at Bembridge) than the previous tie-points used for modelling by Westaway *et al.* (2006). This difference stems partly from the fact that the inner edge of the marine terrace in both modern analogues is higher than mean sea-level, but is exacerbated by the use by Westaway *et al.* (2006) of uncorrected values for the top surface of the overlying deposit, not the inner edge of the marine terrace (Table 1), so that the two elevations are not comparing the same feature. In the case of the WALIS database, none of the datapoints included are comparable with the marine terrace values in this study because there are no marine terrace datapoints listed in this region and the database focuses on last interglacial (Ipswichian Stage) sequences. In addition, the WALIS elevation value from the Brighton–Norton Formation at Norton Farm was taken from the overlying sands and therefore defined as marine limiting rather than a palaeo-RSL value (Table 1; Cohen *et al.* 2022). The WALIS database also lists only a palaeo-RSL from the saltmarsh deposits at Bembridge, not the marine terrace.

New palaeo-RSL values have also been estimated from beach deposits from the MIS 5e Pagham Formation (Table 3), again using the preferred method of modern analogues. This yielded a much wider range of possible palaeo-RSL values (0.3–9.3 m) because of the wide range of elevations at which beach deposits form in the modern coastal system. They overlap with the Kopp *et al.* (2009) estimate of 9.13 m (Table 1), but this latter has an 8 m uncertainty, even larger than the *c.* 4 m uncertainty applied here (Table 3). Again, these cannot be compared with the WALIS database (Cohen *et al.* 2022) because the Pagham Formation deposits are assigned marine limiting status and palaeo-RSL values are not calculated. Although palaeo-RSL values were calculated by WALIS from the Aldingbourne Formation (Table 1), we chose not to do so in this study, given the eroded and dissected nature of these sands and the associated difficulty of direct comparison with modern analogues. It is clear that beach deposits are problematic to use as palaeo-RSL indicators, at least in regions such as southern England with a wide tidal range where modern deposits form over a significant elevation range.

In the WALIS database, sea-level indicators were also calculated from estuarine and saltmarsh sediments at Bembridge and Stone Point on the basis of foraminiferal assemblages interpreted as representing different saltmarsh environments, which are associated with specific elevations (Table 1; Cohen *et al.* 2022). In contrast, we chose not to calculate sea-level indicators from these sequences. This was partly because of the lack of modern analogues in the region at the present day; there are very few salt marshes and those that exist have not been studied in detail. In addition, the sequences from Bembridge and Stone Point are incomplete and it was difficult to assess whether they represented salt marsh deposition at the edge of an estuary or deeper estuarine channel deposition (although the peat beds present at Stone Point may suggest an estuary-edge location). Furthermore, at Stone Point, different fossil groups suggested different salinity levels, presumably owing to tidal transport within the estuary (Briant *et al.* 2019).

We suggest, on the basis of the size of the error margins calculated, that the most reliable palaeo-RSL indicators from the Solent and Sussex coastal plain are those where a marine terrace is preserved, because this has the clearest relationship to local modern analogues, with the smallest error margins. It is hard to compare these new palaeo-RSL values with previous studies because the methods used are very different (Westaway *et al.* 2006; Kopp *et al.* 2009) and the reliability of the different types of indicators has been assessed differently in the WALIS database (Cohen *et al.* 2022), where the salt marsh sequences and beach sequence from the Aldingbourne Formation are designated as sea-level indicators and no marine terraces are included.

Uplift rates

The uplift rates modelled from this study are relatively low, which is not surprising given the lack of evidence for significant tectonic activity since the Miocene (Hopson 2009). Westaway *et al.* (2006) attributed uplift to lower crustal flow from adjacent subsiding areas receiving the erosional products of large river systems such as the Solent into areas from which sediments had been removed. They calculated a range of possible uplift rates, but their favoured solution, based on age estimates for the same tie-points at the same ages as in this study, gave a rate of 0.134 mm a^{-1}. This is only slightly less than the higher uplift rate of 0.164 mm a^{-1} modelled from 485 to *c.* 140 ka in this study and slightly more than a weighted average of the two uplift rates used in this study (*c.* 0.11 mm a^{-1}). It is also very similar to an average uplift value for passive margins globally calculated by Pedoja *et al.* (2011) of 0.13 mm a^{-1}, although Pedoja *et al.* (2014) revised this down to 0.06 mm a^{-1} by including only those datapoints whose elevation falls within the eustatic range of global sea-level compilations. Pedoja *et al.* (2011) and Pedoja *et al.* (2014) both ascribed uplift at passive margins to a gradual increase in the mean compression of the lithosphere inducing deformation and associated uplift. A specific case study of this uplift at passive margins in the Cotentin Peninsula by Pedoja *et al.* (2018) suggested uplift rates of either 0.06 or 0.01 mm a^{-1} using the synchronous correlation method, depending on the age of the four marine terraces observed. Because only the lowest (MIS 5e) terrace is reliably dated in Cotentin, it was not possible to determine uplift rates more precisely. However, for the purposes of comparison, it should be noted that the higher uplift rate of Pedoja *et al.* (2018) coincided with the age model that is most similar to that of the Sussex marine terraces in this study. A sequence of marine terraces is also observed in Jersey (Renouf and James 2011). Elevations cover wide ranges, attributed to the tidal range in Jersey of *c.* 12 m, and absolute age estimates are limited, but uplift rates are tentatively suggested to fall from 0.09 mm a^{-1} at *c.* 500 ka to 0.02 mm a^{-1} at the present day. Neither the Cotentin nor Jersey studies corrected terrace elevations for local indicative meanings, but, nonetheless, uplift rates are similarly low.

The key difference between this study and previous similar studies is that the greater age constraint on the Sussex sequence owing to biostratigraphic age estimates from the Goodwood–Slindon Formation at Boxgrove (Roberts and Parfitt 1999) allows non-uniform uplift rates to be estimated. This may allow the short-term effects of isostatic responses to start to be detected (although not to be fully disentangled from the long-term uplift of the south coastal region without complex ice-sheet and crustal modelling). Generalized compressive uplift could be counteracted significantly by glacioisostatic adjustment (GIA)-related subsidence, given that this reaches *c.* 1.6 mm a^{-1}; for example, in SW England between 0 and 6 ka (Lambeck 1996; Shennan and Horton 2002). Using global positioning system (GPS) corrected modelling, Bradley *et al.* (2009) estimated current (post-Devensian) subsidence in the Sussex and Solent region at *c.* 1.2 mm a^{-1}. Although it is likely that there was considerable variability in uplift rates over the last 485 ka owing to GIA of different magnitudes associated with various ice advances, our modelling suggests that the largest change occurred at *c.* 140 ka (or possibly 160 ka; that is, towards the end of the Late Wolstonian Substage).

A difficulty with estimating subsidence rates for interglacials before the Holocene is that there is insufficient precision in both sea-level estimates and dating of these to determine the location and extent of the forebulge in front of the ice sheet, which is the area that will experience the most subsidence after ice retreat. Busschers *et al.* (2008) suggested that the most extensive Saalian Stage forebulge (i.e. that of the Drenthe Stadial, *c.* 180–160 ka) may have been located between Rotterdam and Amsterdam, further south than Vink *et al.* (2007) placed the Weichselian Stage forebulge (Hijma *et al.* 2012). Alternatively, Hijma *et al.* (2012) and Gibson *et al.* (2022) showed Saalian Stage (Drenthe Stadial) and Wolstonian Stage (Moreton Stadial) ice limits a similar distance from Sussex (*c.* 200 km) to the Devensian and Weichselian Stage limits. Thus similar subsidence rates to those at the present day might have been experienced relating to the Moreton Stadial glacial advance, offsetting compressional uplift associated with a passive margin and leading to the very low uplift rates modelled in this study since *c.* 140 ka. It should be noted, however, that the impact on ground surface level at the time of the associated sea-level transgressions will differ, as the Moreton Stadial advance predates the Ipswichian sea-level highstand by *c.* 40 ka but the Devensian advance by only *c.* 20 ka. In the absence of more detailed modelling it is at the moment only possible to state that subsidence may have occurred owing to forebulge collapse during the penultimate glacial advance in addition to the Devensian advance. This might account for the observed reduced uplift rates in Sussex since *c.* 140 ka (or maybe *c.* 160 ka) by counteracting the underlying long-term uplift rates. Previous work (Bates 2001) has shown that there is a general decrease in numbers of mapped terraces in the river systems from west to east across the region from the Solent to the Adur. This may relate to different glacioisostatic effects causing formation of composite terraces in river systems further east. However, in the absence of absolute age estimates from the Arun and Adur river systems, this cannot be stated with certainty.

Although similar subsidence might also have occurred during the Hoxnian or Holsteinian Stage, following the Elsterian or Anglian glaciation, which reached to within *c.* 100 km of Sussex (Hijma *et al.* 2012), this is harder to determine. This is due to the lack of age constraints in this upper part of the sequence and the presence of only a single marine deposit between the Goodwood–Slindon and Brighton–Norton formations, despite two known global highstand events in this time period.

Overprinting of sea-level events in the landscape

The modelling in Table 5 suggests that the 485 ka (Cromerian Stage or MIS 13) and 405 ka (Hoxnian Stage or MIS 11) highstand events should be seen at the same elevation in the landscape. Recent research has shown that high Hoxnian Stage sea-levels are related to late melting of the Greenland ice sheet (Tzedakis *et al.* 2022), validating the projected elevation estimates in our study. However, there is solid evidence only for one sea-level highstand event at *c.* 38 m, at Boxgrove, where excavations were undertaken in enough detail that evidence from two different events would probably have been seen if it were present. Recent electron spin resonance (ESR) dating of quartz grains from the Slindon Sand at the Valdoe gave mean dates falling within the Hoxnian Stage and the Early Wolstonian Substage (ages coeval with MIS stages 11 and 10), suggesting presence of younger material at Boxgrove, but there are large error margins associated with these dates, meaning that they also overlap with the later part of the Cromerian Stage or MIS 13 (Voinchet *et al.* 2015). In addition, the mammalian biostratigraphic age estimate from Boxgrove is based on the presence of a number of species such as the shrews *Sorex runtonensis* and *Sorex savini*, the cave bear *Ursus deningeri* and the giant deer *Megaloceros dawkinsi* and *M.* cf. *verticornis*, all of which became extinct during the Anglian Stage, *c.* MIS 12 (Roberts and Parfitt 1999).

The lack of evidence of Hoxnian Stage marine sequences may be due to limited quarrying south of the Goodwood–Slindon Formation. Alternatively, their preservation potential may have been low owing to the continuing presence of a closed embayment (Bates *et al.* 2010), forming within clays and silts of the Lambeth and Thames groups (Fig. 1a). Hoxnian Stage deposits would have been preserved only within the embayment, because outside were erosional chalk cliffs, as seen west of Havant and east of the Arun. Preservation potential within the embayment was also likely to be low because the Lambeth and Thames groups south of the Goodwood–Slindon cliffline in the Cretaceous chalk would not readily preserve a marine terrace form because they are significantly erodible. Furthermore, the area to the south of the Goodwood–Slindon Formation would have seen considerable reworking of solifluction deposits overlying the Goodwood–Slindon Formation, which might have also eroded any Hoxnian Stage sands that were deposited.

The Aldingbourne Formation was attributed to MIS 7 (Late Wolstonian Substage) by Bates *et al.* (2010) based on several OSL ages that agree well with each other. However, evidence from unpublished excavations further west, with a very different fauna and independent age estimates, seems more in line with the Middle Wolstonian Substage (*c.* 335 ka highstand, MIS 9) age proposed by the uplift modelling. At present, therefore, the Aldingbourne Formation remains an enigma that requires further investigation but may contain deposits of various ages, including the Middle Wolstonian Substage.

Global sea-level curves place the two Late Wolstonian Substage highstands at 200 and 240 ka at a very similar elevation (Grant *et al.* 2014, Table 5), although assuming constant uplift between these times means that we do not model them at the same elevation in the Sussex sequence. Neither is projected at a significantly higher elevation than the 125 ka highstand, presumably partly because global sea-levels were not particularly high. As discussed above, there is some uncertainty over which highstand is represented in the Brighton–Norton Formation. The key site of Norton Farm has an OSL age from marine sands of *c.* 240 ka but the mammalian biostratigraphy suggests a *c.* 200 ka age (Bates *et al.* 2000). The OSL age from the marine sands of *c.* 240 ka (Bates *et al.* 2010) has large error bars of *c.* 30 ka, which may reflect either inclusion of older sediments and associated incomplete bleaching of the sample or insufficiently detailed dose rate determination because the sample was taken from a borehole. The horse found in marine sands and overlying terrestrial silts at Norton Farm is a particularly small form of *Equus ferus,* previously seen only in deposits attributed to late MIS 7 and the early part of MIS 6; that is, within the Late Wolstonian Substage (Parfitt 1998). Candy and Schreve (2007) later refined the dating of this small horse to early in the Late Wolstonian Substage glacial period (*c.* MIS 6) at Marsworth, where it was recorded in slope deposits overlying precisely dated tufa deposits within an underlying channel that contained full-size horse remains (Murton *et al.* 2001). Bates *et al.* (2010) concluded that the dating evidence is insufficient to differentiate between these two highstands at this site.

This age uncertainty raises the possibility that the Brighton–Norton Formation at Norton Farm is a composite sequence, forming during both 240 and 200 ka highstand events. The modelling results in this study suggest that the marine terrace itself was most probably formed at the 240 ka highstand, but it is possible that the sedimentary sequence overlying it may date at least partially from 200 ka. The original investigation of the Brighton–Norton Formation at Norton Farm showed that it represented a period of marine regression, grading upwards from marine sands into terrestrial silts (Fig. 4) with pollen and molluscs suggesting a cool or cold climate throughout. Foraminiferal and ostracod data show marine elements throughout, whereas the molluscs contain more freshwater elements (Bates *et al.* 2000). The terrestrial elements seen in this sequence and related sequences at Tangmere and Portfield Pit (Bates *et al.* 2010) might corroborate the slightly lower modelled sea-level for the 200 ka highstand in this study. It therefore seems likely that at *c.* 240 ka a shallow terrace formed both in Cretaceous chalk and in the Thames and Lambeth Group rocks southward of the Brighton–Norton cliffline on which a range of marine sediments were deposited during the 200 ka highstand near Norton Farm and then again during the 125 ka highstand further south.

Controls on preservation of robust relative sea-level indicators

It is striking that marine terraces have been preserved only in more competent rocks: Cretaceous chalk at Boxgrove and Norton Farm and Bembridge Limestone at Bembridge. The presence of more erodible Eocene rocks of the Thames and Lambeth groups interspersed with chalk on the Sussex coastal plain has led to a gap in the record of sea-level change for the Hoxnian Stage (see above), a patchy record of the Aldingbourne Formation, tentatively assigned by modelling in this study to the Middle Wolstonian Substage (*c.* 335 ka highstand) and a wide range of elevation estimates for past sea-level during the Ipswichian Stage from the Pagham Formation.

Whereas at Bembridge a clear marine terrace formed in Bembridge Limestone during the Ipswichian Stage, this was not the case further east. In Sussex, the lack of a clear cliffline associated with the Pagham Formation is exacerbated by both the similarity of the highstand elevation to that of the 240 and 200 ka highstands and a change in bedrock lithology. At the start of the Ipswichian Stage, the geomorphology of the Sussex coastline probably comprised a relict marine terrace formed in Cretaceous chalk to the north, with 5–10 m of slope deposits overlying marine sands, showing a transition southwards into a terrace formed in the Thames and Lambeth Groups. It is plausible that the 125 ka highstand transgressed over this platform, depositing the beach sediments known as the Pagham Formation, but was unable to form a new preservable marine terrace owing to a lack of suitable rocks to erode. The Ipswichian Stage beach deposits probably abutted directly onto slope deposits, as seen at Portelet and Belcroute in Jersey and also in the Cotentin Peninsula of northern France (Renouf and James 2011), although such direct relationships have not been seen in Sussex.

This marks a significant shift in coastal configuration during the Ipswichian Stage. A relatively stable coastline position persisted from the Cromerian Stage to the Middle Wolstonian Substage (*c.* MIS 13 to MIS 9), backed by the Cretaceous chalk ridge (with the single large Goodwood–Slindon bay). This would have altered significantly when the coastline shifted southwards onto the Eocene deposits. Coupled with lower rates of uplift this shift in bedrock types created the opportunity for the development of the harboured coastline postulated by Bates *et al.* (2010), where packages of sediments from both the Ipswichian Stage and Late Wolstonian Substages (*c.* MIS 5e and 7, and 125, 200 and 240 ka highstands) seem to occupy similar elevations in the landscape. The different distributions of the softer Eocene and harder chalk bedrocks across this coastal plain probably further enhanced this complexity by responding differently to periglacial activity during cold periods, creating shallow water bodies during cold stages, subsequently exploited by the sea during the following highstand episode. This led to dissection of the Pagham Formation and replacement with a series of cold stage and Holocene silts; for example, at Warblington (Fig. 3b; Bates *et al.* 2009*b*; Bates *et al.* 2010).

Interactions with the fluvial systems of the Lavant to the west and Arun to the east also reduce the preservation potential of Pagham Formation sequences. Although the most significant evidence of Lavant activity is in the Chichester Fan Gravels on which the town of Chichester has been built (Fig. 1b), the interglacial channels around Selsey Bill also appear to be associated with channels emerging from the Lavant Valley. These channels were probably cut during one or more cold stages and then filled during various interglacial transgressions. Sequences are thought to become progressively younger from west to east from Earnley to West Wittering, West Street Selsey and the Lifeboat station channel to the east of Selsey Bill (Briant *et al.* 2022). To the east, the Arun channel cuts fully across the marine terrace, with probably further dissection from tributary valleys running east–west as at the present day. Pagham Formation marine deposits were therefore deposited across a marine terrace that was dissected by river channels as well as differential periglacial wasting of different bedrock types, significantly reducing their preservation potential.

Conclusions

This study provides three new robust palaeo-RSL datapoints from marine terraces for the Solent and Sussex region in southern England, based on correction for indicative meanings from modern analogues. Palaeo-RSL values were also calculated from beach deposits of the Pagham Formation, but these are not reliable enough to use to determine past sea-level. The new palaeo-RSL datapoints in this study are different from, but not directly comparable with, previous palaeo-RSL estimates from this region.

The marine terrace palaeo-RSL values are as follows: (1) Goodwood–Slindon Formation at Boxgrove: 37.5 ± 1.7 m (age of late Cromerian Stage based on biostratigraphy, *c.* MIS 13 or 485 ka highstand); (2) Brighton–Norton Formation at Norton Farm: 5.7 ± 1.8 m (age of Late Wolstonian Substage or MIS 7, either 200 ka or 240 ka highstand; OSL and biostratigraphy conflict); (3) Bembridge: 5.3 ± 2 m (age of Ipswichian Stage, *c.* MIS 5e or 125 ka based on OSL).

Modelling uplift based on the two palaeo-RSL datapoints with the most reliable age estimates (Boxgrove and Bembridge) suggests the following conclusions.

(1) Uplift rates are low, and comparable with those found in other passive margin settings (i.e. noticeably below 0.2 mm a^{-1}).
(2) Uplift rates are modelled to have changed at *c.* 140 ka, modelled at 0.164 mm a^{-1} between 485 and 140 ka and 0.005 mm a^{-1} afterwards. It is suggested that the reduction in uplift rate might be due to compressive uplift being offset by GIA subsidence, although this cannot be confirmed without more detailed crustal and GIA modelling.
(3) The 405 ka highstand of the Hoxnian Stage (*c.* MIS 11) is modelled to be coincident with that of the earlier 485 ka highstand, but no evidence is found in the landscape of this event, possibly because of the thick covering of slope deposits above the Goodwood–Slindon Formation or the geomorphological setting.
(4) The Aldingbourne Formation at an elevation of *c.* 21 m OD (uncorrected) coincides with a modelled highstand at *c.* 335 ka, during the Middle Wolstonian Substage. If accurate, this would place it earlier in time than previously suggested by OSL dating.
(5) The Brighton–Norton Formation marine terrace at Norton Farm deposited within the Late Wolstonian Substage is modelled to *c.* 240 ka, suggesting that the overlying sediments whose age has been suggested as late MIS 7 (i.e. similar to the 200 ka highstand) might have been emplaced on a pre-existing geomorphological feature.
(6) The only marine terrace preserved from the Ipswichian Stage (*c.* 125 ka highstand) is at Bembridge on the Isle of Wight. It is suggested that this is due to the underlying bedrock being stronger than the bedrock underlying the Pagham Formation in Sussex. Preservation potential of the Pagham Formation has been further reduced by differential periglacial wasting of different bedrock types and fluvial dissection.

Scientific editing by Philip Hughes

Acknowledgements We would like to thank all the landowners on whose land we have drilled, dug and investigated. We are grateful to K. Pedoja and an anonymous reviewer whose comments on an earlier draft of this paper greatly improved it. A CC BY or equivalent licence is applied to the authors' accepted manuscript (AAM) arising from this submission.

Author contributions **RMB**: conceptualization (lead), data curation (equal), formal analysis (equal), investigation (equal); **MRB**: conceptualization (equal), data curation (equal), formal analysis (equal), funding acquisition (lead), investigation (lead); **JR**: formal analysis (equal); **J-LS**: formal analysis (supporting); **JEW**: formal analysis (supporting)

Funding Research described in this paper was funded from multiple sources, including archaeological consultancy work and an English Heritage funded Aggregate Levy Sustainability Fund project (*Palaeolithic Archaeology of the Sussex/Hampshire Coastal Corridor* Phases I and II, 3709) that covered much of the field and laboratory costs incurred in elements of the project.

Competing interests The authors declare that they have no known competing financial interests or personal relationships that could have appeared to influence the work reported in this paper.

Data availability All data generated or analysed during this study are included in this published article and its supplementary information file.

References

Allen, L.G. and Gibbard, P.L. 1993. Pleistocene evolution of the Solent River of southern England. *Quaternary Science Reviews*, **12**, 503–528, https://doi.org/10.1016/0277-3791(93)90067-V

Allen, L.G., Gibbard, P.L., Pettit, M.E., Preece, R.C. and Robinson, J.E. 1996. Late Pleistocene interglacial deposits at Pennington Marshes, Lymington, Hampshire, southern England. *Proceedings of the Geologists' Association*, **107**, 39–50, https://doi.org/10.1016/S0016-7878(96)80066-6

Bates, M.R. 2001. The Meeting of the Waters: raised beaches and river gravels of the Sussex Coastal Plain/Hampshire Basin. *Lithic Studies Society Occasional Paper*, **7**, 27–45.

Bates, M.R., Bates, C.R. *et al.* 2000. Late Middle Pleistocene deposits at Norton Farm on the West Sussex coastal plain, southern England. *Journal of Quaternary Science*, **15**, 61–89, https://doi.org/10.1002/(SICI)1099-1417(200001)15:1<61::AID-JQS463>3.0.CO;2-K

Bates, M.R., Keen, D.H. and Lautridou, J.P. 2003. Pleistocene marine and periglacial deposits of the English Channel. *Journal of Quaternary Science*, **18**, 319–337, https://doi.org/10.1002/jqs.747

Bates, M.R., Wenban-Smith, F.F., Briant, R.M. and Marshall, G. 2004. *Palaeolithic Archaeology of the Sussex/Hampshire Coastal Corridor*. English Heritage Archive Report, Project No. **3279**.

Bates, M.R., Bates, C.R. *et al.* 2009*a*. West Street, Selsey. *In*: Briant, R.M., Bates, M.R., Hosfield, R.T. and Wenban-Smith, F.F. (eds) *The Quaternary of the Solent Basin and West Sussex Raised Beaches. Field Guide*. Quaternary Research Association, London, 73–95.

Bates, M.R., Bates, C.R., Bates, S., Jones, S., Schwenninger, J.-L., Walker, M.J.C. and Whittaker, J.E. 2009*b*. Cold stage deposits of the West Sussex Coastal Plain: the evidence from Warblington, Hampshire. *In*: Briant, R.M.,

Bates, M.R., Hosfield, R.T. and Wenban-Smith, F.F. (eds) *The Quaternary of the Solent Basin and West Sussex Raised Beaches. Field Guide*. Quaternary Research Association, London, 60–72.
Bates, M.R., Briant, R.M., Rhodes, E.J., Schwenninger, J.L. and Whittaker, J.E. 2010. A new chronological framework for Middle and Upper Pleistocene landscape evolution in the Sussex/Hampshire Coastal Corridor. *Proceedings of the Geologists' Association*, **121**, 369–392, https://doi.org/10.1016/j.pgeola.2010.02.004
Bates, S.L., Siddall, M. and Waelbroeck, C. 2014. Hydrographic variations in deep ocean temperature over the mid-Pleistocene transition. *Quaternary Science Reviews*, **88**, 147–158, https://doi.org/10.1016/j.quascirev.2014.01.020
Bates, M.R., Bates, C.R., Toms, P., Krawiec, K. and Pope, M. 2019. Medmerry and the Manhood Peninsula in its Quaternary context. *In*: Stephenson, P. and Krawiec, K. (eds) *A View from the Edge: Archaeological Investigation on the Manhood Peninsula, Selsey for the Medmerry Managed Realignment Scheme*. SpoilHeap Publications. University College London, London, 15–27.
Bintanja, R., Van De Wal, R.S. and Oerlemans, J. 2005. Modelled atmospheric temperatures and global sea levels over the past million years. *Nature*, **437**, 125–128, https://doi.org/10.1038/nature03975
Bowen, D.Q. 1999. *A Revised Correlation of Quaternary Deposits in the British Isles*. Geological Society, London, Special Report, **23**.
Bradley, S.L., Milne, G.A., Teferle, F.N., Bingley, R.M. and Orliac, E.J. 2009. Glacial isostatic adjustment of the British Isles: new constraints from GPS measurements of crustal motion. *Geophysical Journal International*, **178**, 14–22, https://doi.org/10.1111/j.1365-246X.2008.04033.x
Briant, R.M., Bates, M.R., Schwenninger, J.-L. and Wenban-Smith, F.F. 2006. A long optically-stimulated luminescence dated Middle to Late Pleistocene fluvial sequence from the western Solent Basin, southern England. *Journal of Quaternary Science*, **21**, 507–523, https://doi.org/10.1002/jqs.1035
Briant, R.M., Bates, M.R. *et al.* 2009. Gravels and interglacial sediments at Stone Point Site of Special Scientific Interest, Lepe Country Park, Hampshire. *In*: Briant, R.M., Bates, M.R., Hosfield, R.T. and Wenban-Smith, F.F. (eds) *The Quaternary of the Solent Basin and West Sussex Raised Beaches. Field Guide*. Quaternary Research Association, London, 171–188.
Briant, R.M., Bates, M.R. *et al.* 2013. Palaeoenvironmental reconstruction from a decalcified interglacial sequence in the former Solent rivers system at St Leonard's Farm, Hampshire, England. *Quaternary Newsletter*, **130**, 23–40.
Briant, R.M., Bates, M.R. *et al.* 2019. Early Ipswichian (last interglacial) sea level rise in the channel region: Stone Point Site of Special Scientific Interest, Hampshire, England. *Proceedings of the Geologists' Association*, **130**, 1–26, https://doi.org/10.1016/j.pgeola.2018.03.002
Briant, R.M., Haggart, B.A., Schreve, D.C. and Whiteman, C.A. 2022. Quaternary sea level landforms and sediments in southern England: description of geological conservation review sites. *Proceedings of the Geologists' Association*, https://doi.org/10.1016/j.pgeola.2022.06.
Brown, R.C., Gilbertson, D.D., Green, C.P. and Keen, D.H. 1975. Stratigraphy and environmental significance of Pleistocene deposits at Stone, Hampshire. *Proceedings of the Geologists' Association*, **86**, 349–363, https://doi.org/10.1016/S0016-7878(75)80026-5
Busschers, F.S., Kasse, C. *et al.* 2008. Late Pleistocene evolution of the Rhine–Meuse system in the southern North Sea basin: imprints of climate change, sea-level oscillation and glacio-isostacy. *Quaternary Science Reviews*, **26**, 3216–3248, https://doi.org/10.1016/j.quascirev.2007.07.013
Candy, I. and Schreve, D. 2007. Land–sea correlation of Middle Pleistocene temperate sub-stages using high-precision uranium-series dating of tufa deposits from southern England. *Quaternary Science Reviews*, **26**, 1223–1235, https://doi.org/10.1016/j.quascirev.2007.01.012
Caputo, R. 2007. Sea-level curves: perplexities of an end-user in morphotectonic applications. *Global and Planetary Change*, **57**, 417–423, https://doi.org/10.1016/j.gloplacha.2007.03.003
Channel Coast Observatory 2021. Data available from https://coastalmonitoring.org/cco/ [last accessed 31 July 2021].
Cohen, K.M., Cartelle, V., Barnett, R., Busschers, F.S. and Barlow, N.L. 2022. Last Interglacial sea-level data points from Northwest Europe. *Earth System Science Data*, **14**, 2895–2937, https://doi.org/10.5194/essd-14-2895-2022
De Gelder, G., Jara-Muñoz, J. *et al.* 2020. How do sea-level curves influence modelled marine terrace sequences? *Quaternary Science Reviews*, **229**, 106132, https://doi.org/10.1016/j.quascirev.2019.106132
De Santis, V., Scardino, G. *et al.* 2023. Middle–late Pleistocene chronology of palaeoshorelines and uplift history in the low-rising to stable Apulian foreland: overprinting and reoccupation. *Geomorphology*, **421**, 108530, https://doi.org/10.1016/j.geomorph.2022.108530
Gale, A. 2019. *The Isle of Wight.* Geologists' Association Field Guide, **60**.
Gibbard, P.L. 1988. The history of the great northwest European rivers during the past three million years. *Philosophical Transactions of the Royal Society of London, Series B*, **318**, 559–602, https://doi.org/10.1098/rstb.1988.0024
Gibbard, P.L. 1995. The formation of the Strait of Dover. *Geological Society, London, Special Publications*, **96**, 15–26, https://doi.org/10.1144/GSL.SP.1995.096.01.03
Gibbard, P.L. and Hughes, P.D. 2021. Terrestrial stratigraphical division in the Quaternary and its correlation. *Journal of the Geological Society, London*, **178**, jgs2020-134, https://doi.org/10.1144/jgs2020-134
Gibson, S.M., Bateman, M.D., Murton, J.B., Barrows, T.T., Fifield, L.K. and Gibbard, P.L. 2022. Timing and dynamics of Late Wolstonian Substage 'Moreton Stadial' (MIS 6) glaciation in the English West Midlands, UK. *Royal Society Open Science*, **9**, 220312, https://doi.org/10.1098/rsos.220312
Grant, K.M., Rohling, E.J. *et al.* 2014. Sea-level variability over five glacial cycles. *Nature Communications*, **5**, https://doi.org/10.1038/ncomms6076
Gupta, S., Collier, J.S., Palmer-Felgate, A. and Potter, G. 2007. Catastrophic flooding origin of shelf valley systems in the English Channel. *Nature*, **448**, 342–345, https://doi.org/10.1038/nature06018
Hijma, M.P., Cohen, K.M., Roebroeks, W., Westerhoff, W.E. and Busschers, F.S. 2012. Pleistocene Rhine–Thames landscapes: geological background for hominin occupation of the southern North Sea region. *Journal of Quaternary Science*, **27**, 17–39, https://doi.org/10.1002/jqs.1549
Hopson, P.M. 2009. The geological setting of the coastal fringes of West Sussex, Hampshire and the Isle of Wight. *In*: Briant, R.M., Bates, M.R., Hosfield, R.T. and Wenban-Smith, F.F. (eds) *The Quaternary of the Solent Basin and West Sussex Raised Beaches. Field Guide*. Quaternary Research Association, London, 1–20.
Houghton, S.L., Roberts, G.P., Papanikolaou, I.D., McArthur, J.M. and Gilmour, M.A. 2003. New ^{234}U–^{230}Th coral dates from the western Gulf of Corinth: implications for extensional tectonics. *Geophysical Research Letters*, **30**, 19, https://doi.org/10.1029/2003GL018112
Jara-Muñoz, J. and Melnick, D. 2015. Unraveling sea-level variations and tectonic uplift in wave-built marine terraces, Santa María Island, Chile. *Quaternary Research*, **83**, 216–228, https://doi.org/10.1016/j.yqres.2014.10.002
Kopp, R.E., Simons, F.J., Mitrovica, J.X., Maloof, A.C. and Oppenheimer, M. 2009. Probabilistic assessment of sea-level during the last interglacial stage. *Nature*, **462**, 863–867, https://doi.org/10.1038/nature08686
Lambeck, K. 1996. Glaciation and sea-level change for Ireland and the Irish Sea since Late Devensian/Midlandian time. *Journal of the Geological Society, London*, **153**, 853–872, https://doi.org/10.1144/gsjgs.153.6.0853
Lisiecki, L.E. and Raymo, M.E. 2005. A Pliocene–Pleistocene stack of 57 globally distributed benthic δ^{18}O records. *Paleoceanography*, **20**, https://doi.org/10.1029/2004PA001071
Long, A.J., Barlow, N.L., Busschers, F.S., Cohen, K.M., Gehrels, W.R. and Wake, L.M. 2015. Near-field sea-level variability in northwest Europe and ice sheet stability during the last interglacial. *Quaternary Science Reviews*, **126**, 26–40, https://doi.org/10.1016/j.quascirev.2015.08.021
Lorscheid, T. and Rovere, A. 2019. The indicative meaning calculator – quantification of paleo sea-level relationships by using global wave and tide datasets. *Open Geospatial Data, Software and Standards*, **4**, 10, https://doi.org/10.1186/s40965-019-0069-8
Melville, R.V. and Freshney, E.C. 1982. *The Hampshire Basin and Adjoining Area*, 4th edn. HMSO, London.
Meschis, M., Roberts, G.P., Robertson, J. and Briant, R.M. 2018. The relationships between regional Quaternary uplift, deformation across active normal faults, and historical seismicity in the upper plate of subduction zones: the Capo D'Orlando fault, NE Sicily. *Tectonics*, **37**, 1231–1255, https://doi.org/10.1029/2017TC004705
Murton, J.B., Baker, A. *et al.* 2001. A late Middle Pleistocene temperate–periglacial–temperate sequence (Oxygen Isotope Stages 7–5e) near Marsworth, Buckinghamshire, UK. *Quaternary Science Reviews*, **20**, 1787–1825, https://doi.org/10.1016/S0277-3791(01)00004-X
New Forest District Council 2017. 2012 Update of Carter, D., Bray, M., and Hooke, J., 2004 SCOPAC Sediment Transport Study, www.scopac.org.uk/sts [last accessed 30 November 2022].
Normand, R., Simpson, G., Herman, F., Biswas, R.H., Bahroudi, A. and Schneider, B. 2019. Dating and morpho-stratigraphy of uplifted marine terraces in the Makran subduction zone (Iran). *Earth Surface Dynamics*, **7**, 321–344, https://doi.org/10.5194/esurf-7-321-2019
Parfitt, S.A. 1998. Pleistocene vertebrates of the West Sussex Coastal Plain: their stratigraphic and palaeoenvironmental significance. *In*: Murton, J.B., Whiteman, C.A., Bates, M.R., Bridgland, D.R., Long, A.J. Roberts, M.B. and Waller, M.P. (eds) *The Quaternary of Kent and Sussex. Field Guide*. Quaternary Research Association, London, 121–135.
Parks, D.A. and Rendell, H.M. 1992. Thermoluminescence dating and geochemistry of loessic deposits in southeast England. *Journal of Quaternary Science*, **7**, 99–107.
Past Interglacials Working Group of PAGES 2016. Interglacials of the last 800,000 years. *Reviews of Geophysics*, **54**, 162–219, https://doi.org/10.1002/2015RG000482
Pedoja, K., Husson, L. *et al.* 2011. Relative sea-level fall since the last interglacial stage: are coasts uplifting worldwide? *Earth-Science Reviews*, **108**, 1–15, https://doi.org/10.1016/j.earscirev.2011.05.002
Pedoja, K., Husson, L. *et al.* 2014. Coastal staircase sequences reflecting sea-level oscillations and tectonic uplift during the Quaternary and Neogene. *Earth-Science Reviews*, **132**, 13–38, https://doi.org/10.1016/j.earscirev.2014.01.007
Pedoja, K., Jara-Muñoz, J. *et al.* 2018. Neogene–Quaternary slow coastal uplift of Western Europe through the perspective of sequences of strandlines from the Cotentin Peninsula (Normandy, France). *Geomorphology*, **303**, 338–356, https://doi.org/10.1016/j.geomorph.2017.11.021
Plint, A.G. 1982. Eocene sedimentation and tectonics in the Hampshire Basin. *Journal of the Geological Society, London*, **139**, 249–254, https://doi.org/10.1144/gsjgs.139.3.0249
Preece, R.C., Scourse, J.D., Houghton, S.D., Knudsen, K.L. and Penny, D.N. 1990. The Pleistocene sea-level and neotectonic history of the eastern Solent,

Southern England. *Philosophical Transactions of the Royal Society of London, Series B*, **328**, 425–477.

Renouf, J. and James, L. 2011. High level shore features of Jersey (Channel Islands) and adjacent areas. *Quaternary International*, **231**, 62–77, https://doi.org/10.1016/j.quaint.2010.07.005

Rixhon, G., Briant, R.M., Cordier, S., Duval, M., Jones, A. and Scholz, D. 2017. Revealing the pace of river landscape evolution during the Quaternary: recent developments in numerical dating methods. *Quaternary Science Reviews*, **166**, 91–113, https://doi.org/10.1016/j.quascirev.2016.08.016

Roberts, G.P., Houghton, S.L. *et al.* 2009. Localization of Quaternary slip rates in an active rift in 105 years: an example from central Greece constrained by $^{234}U/^{230}Th$ coral dates from uplifted paleoshorelines. *Journal of Geophysical Research*, **114**, B10406, https://doi.org/10.1029/2008JB005818

Roberts, G.P., Meschis, M., Houghton, S., Underwood, C. and Briant, R.M. 2013. The implications of revised Quaternary paleoshoreline chronologies for the rates of active extension and uplift in the upper plate of subduction zones. *Quaternary Science Reviews*, **78**, 169–187, https://doi.org/10.1016/j.quascirev.2013.08.006

Roberts, M.B. and Parfitt, S.A. 1999. *Boxgrove. A Middle Pleistocene Hominid Site at Eartham Quarry, Boxgrove, West Sussex*. English Heritage *Archaeological Report*, **17**.

Robertson, J., Meschis, M., Roberts, G.P., Ganas, A. and Gheorghiu, D.M. 2019. Temporally constant Quaternary uplift rates and their relationship with extensional upper-plate faults in south Crete (Greece), constrained with ^{36}Cl cosmogenic exposure dating. *Tectonics*, **38**, 1189–1222, https://doi.org/10.1029/2018TC005410

Rohling, E.J., Foster, G.L., Grant, K.M., Marino, G., Roberts, A.P., Tamisiea, M.E. and Williams, F. 2014. Sea-level and deep-sea-temperature variability over the past 5.3 million years. *Nature*, **508**, 477–482, https://doi.org/10.1038/nature13230

Rovere, A., Raymo, M.E. *et al.* 2016. The analysis of Last Interglacial (MIS 5e) relative sea-level indicators: reconstructing sea-level in a warmer world. *Earth-Science Reviews*, **159**, 404–427, https://doi.org/10.1016/j.earscirev.2016.06.006

Shennan, I. and Horton, B. 2002. Holocene land- and sea-level changes in Great Britain. *Journal of Quaternary Science*, **17**, 511–526, https://doi.org/10.1002/jqs.710

Siddall, M., Rohling, E.J., Almogi-Labin, A., Hemleben, C., Meischner, D., Schmelzer, I. and Smeed, D.A. 2003. Sea-level fluctuations during the last glacial cycle. *Nature*, **423**, 853–858, https://doi.org/10.1038/nature01690

Spratt, R.M. and Lisiecki, L.E. 2016. A Late Pleistocene sea level stack. *Climates of the Past*, **12**, 1079–1092, https://doi.org/10.5194/cp-12-1079-2016

Tzedakis, P.C., Hodell, D.A., Nehrbass-Ahles, C., Mitsui, T. and Wolff, E.W. 2022. Marine isotope stage 11c: an unusual interglacial. *Quaternary Science Reviews*, **284**, 107493, https://doi.org/10.1016/j.quascirev.2022.107493

Vink, A., Steffen, H., Reinhardt, L. and Kaufmann, G. 2007. Holocene relative sea-level change, isostatic subsidence and the radial viscosity structure of the mantle of northwest Europe (Belgium, the Netherlands, Germany, southern North Sea). *Quaternary Science Reviews*, **26**, 3249–3275, https://doi.org/10.1016/j.quascirev.2007.07.014

Voinchet, P., Moreno, D. *et al.* 2015. New chronological data (ESR and ESR/U-series) for the earliest Acheulian sites of north-western Europe. *Journal of Quaternary Science*, **30**, 610–622, https://doi.org/10.1002/jqs.2814

Wenban-Smith, F.F., Schwenninger, J.-L. and Scaife, R. 2005. New OSL dates and pollen records from the Bembridge Raised Beach sequence, Isle of Wight (UK). *Quaternary Newsletter*, **107**, 1–19.

West, R.G. and Sparks, B.W. 1960. Coastal interglacial deposits of the English Channel. *Philosophical Transactions of the Royal Society of London*, **243**, 95–133.

Westaway, R.W.C., Bridgland, D.R. and White, M. 2006. The Quaternary uplift history of central southern England: evidence from the terraces of the Solent River system and nearby raised beaches. *Quaternary Science Reviews*, **25**, 2212–2250, https://doi.org/10.1016/j.quascirev.2005.06.005